Development of an innovative drug delivery system targeted to adipose vessel utilizing novel nucleic acid aptamer for control of obesity

(新規核酸アプタマーを用いた脂肪血管標的化ナノ送達システムの開発)

A Dissertation Submitted to Hokkaido University for the Partial Fulfillment of the Requirements of the Degree of Doctor of Pharmaceutical Sciences

Supervisor

Professor Dr. Hideyoshi Harashima

SUBMITTED BY

Mahmuda Nargis

Laboratory of Innovative Nanomedicine

Biomedical and Pharmaceutical Science Course

Graduate School of Life Science

Hokkaido University, Japan

August, 2014

DEDICATED TO MY PARENTS AND FAMILY

Acknowledgements

The studies of this dissertation has been carried out in the Laboratory of Innovative Nanomedicine, Department of Pharmaceutical Sciences, Graduate School of Life Science, Hokkaido University during 2011-2014, under the supervision of **Professor Dr. Hideyoshi Harashima.**

My very sincere thanks first goes to Almighty Allah, who has generously gifted me the ability to conduct the research work and knowledge to understand Pharmaceutical Science for writing this dissertation.

I am eager to express my most sincere thankfulness to some invaluable people who made this work possible. My sincere gratitude and appreciation go to my academic supervisor **Professor Dr. Hideyoshi Harashima**, Faculty of Pharmaceutical Sciences, Hokkaido University, Hokkaido, for his friendly cooperation, meticulous attention, productive suggestions and continual guidance during the course of this work. I gratefully acknowledge his assiduous effort, perseverance, enthusiasm and kindness to continue this work without which the present achievement might not have been materialized. I am fortunate enough to have been influenced by his approach to research, which embodies all the best of collegiality and the true spirit of scientific endeavor. I would next like to express my cordial thanks to **Dr.**

Kazuaki Kajimoto, Laboratory of Innovative Nanomedicine, Faculty of Pharmaceutical Sciences, Hokkaido University, Hokkaido, for his valuable comments, constructive criticisms and noteworthy inspiration during the course of experiments which helped to resolve many critical points related to this work. I am highly obliged to **Dr. Hidetaka Akita**, Faculty of Pharmaceutical Sciences, Hokkaido University, Hokkaido, and **Dr. Mamoru Hyodo**, Faculty of Pharmaceutical Sciences, Hokkaido University, Hokkaido, for their helpful co-operation. I feel proud, by way of their benignity and inspiration; have tied me for life with unforgettable sweet memories.

I am indebted to all of my former and present lab mates for their amazing complaisance and co-operation not only in my research work, but also to the every span of my life in Japan. I do not have the courage to further mention some by names for the fear of perplexing omission. Cordial thanks to all of my well-wishers for their amicable co-operation and incentive.

Finally, I am eternally grateful to my parents and my brother for their forever love and support.

(Mahmuda Nargis)

Contents

Chapter 1

Introduction

1
Introduction

1.1. Obesity

Obesity is a growing complex condition that is the serious public health problem worldwide. It affects almost all age and socioeconomic groups and threatens both developed and developing countries [1, 2]. Obesity and overweight is defined, as the accumulation of excessive fat in body mass and considered when body mass index of a person is ≥30 or 25-29.9 respectively [2, 3].

In 1995, World Health Organization (WHO) categorized 200 million adults as obese and 18 million under-five children as overweight worldwide. The number of obese adults increased over 300 million, in 2000. It is predicted that approximately 2·3 billion adults will be overweight or obese by the year 2015 (WHO 2005).

Obesity is highly correlated with various life threatening diseases like, heart disease, diabetes, sleep apnea, certain types of cancer, osteoarthritis and so on [4- 7] (**Figure 1.1**). Obesity is categorized as disease by the American Medical Association in 2013[8, 9].

Figure 1.1: Obesity and its related diseases.

1.2. Management of obesity

Obesity is a preventable medical condition, which can be controlled by following ways-

I. Physical control and

II. Therapeutic control

I. Physical control

Obesity is mainly controlled by dieting and physical exercises [10]. Person having obesity and overweight has to maintain strict diet chart and hard exercise. Maintaining the regular diet program is normally difficult and often a person requires following these lifestyles permanently [11, 12]. Very low calorie containing diet and hard exercise cause various adverse effects like increase risk of gout, loss of lean muscle mass, electrolyte imbalance. Person following these life style must be monitored by a physician to prevent difficulties [13]. However, the success rates for maintaining long-term weight loss with lifestyle changes are low, ranging from 2–20% [14].

Bariatric surgery is the most effective treatment for obesity. This surgery is only recommended for severely obese people (BMI > 40), due to several complications after surgery [15].

II. Therapeutic control

There are only few therapeutic agents (orlistat, sibutramine, lorcaserin, phentermine-topiramate) that can reduce body weight by decreasing the consumption or absorption of food or by increasing energy expenditure[16, 17]. Unfortunately, these drugs have limited success for controlling body weight and most of them have been withdrawn due to their severe adverse effect[18] (**Table 1.1**).

Table 1.1: Antiobesity drugs with their mechanism of action and side effects

Drugs	Market name	Working mechanism	Side effects
Orlistat	Xenical	Reduces intestinal fat absorption by inhibiting pancreatic lipase	Stomach pain, gas, diarrhea, and leakage of oily stools.
Lorcaserin	Belviq	Acts on the serotonin receptors in the brain	Headaches, dizziness, feeling tired, nausea, dry mouth, cough, and constipation.
Phentermine - topiramate	Qsymia	Phentermine (suppresses your appetite and curbs your desire to eat) and topiramate (used to treat seizures or migraine headaches	Tingling of hands and feet, dizziness, taste alterations (particularly with carbonated beverages), trouble sleeping, constipation, and dry mouth.

The limitations of obesity drugs, current situations of obesity and its related diseases demand the detail study for the better understanding of the obesity development and the safe and effective new therapeutic approaches for controlling obesity.

1.3. Adipose tissue

Obesity and its related diseases are directly connected with the microenvironment of adipose tissue [19]. Adipose tissue displays a remarkable plasticity and constitutes one of the few tissues with the ability to considerably expand or regress in adulthood. It is a loose connective tissue, which is found in several parts of the body with two different forms- white adipose tissue and brown adipose tissue. White adipose tissue contributes the major part in the body and is considered for the responsible of obesity development.

White adipose tissue mainly composed of adipocytes, and stromal- cells (vascular endothelial cells, macrophages and stem cells). All adipocytes are encircled by microvessels, which play important role in adipose tissue by providing oxygen and nutrients [20] (**Figure 1.2**).

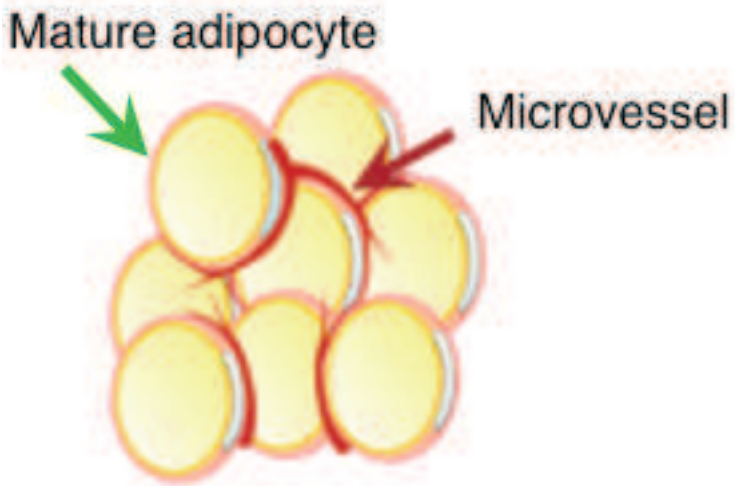

Figure 1.2: Adipose tissue and vasculature.

1.4. Growth of adipose tissue

The growth of adipose tissue depends on continuous remodeling of the vascular network (angiogenesis). Expansion of adipose tissue can be supported by both neovascularization and dilation and remodeling of existing capillaries. During development of adipose tissue different types of angiogenic factors such as vascular endothelial growth factor (VEGF), matrix metalloproteinases (MMPs) release from macrophages into adipose tissue. These factors then stimulate the formation of new blood vessels [20] (**Figure 1.3**).

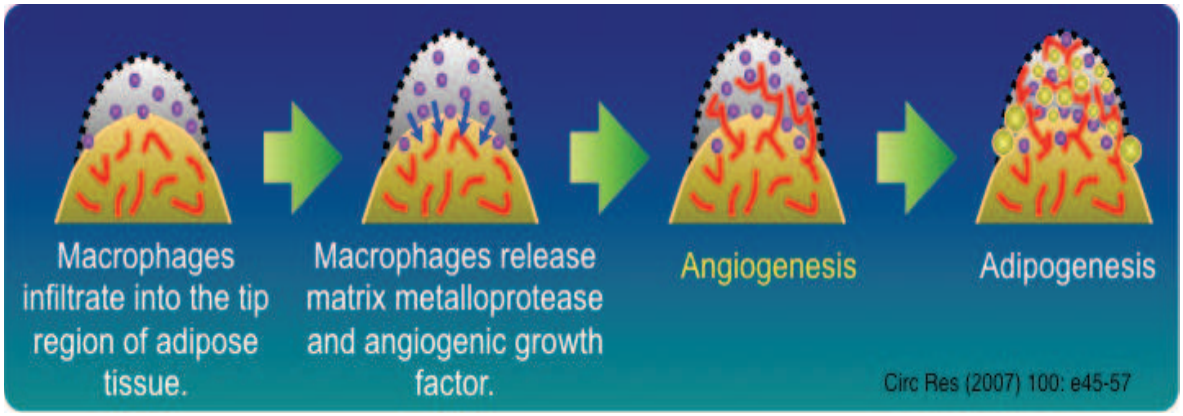

Figure 1.3: Angiogenesis dependent adipogenesis. Infiltration of macrophages into the tip region of adipose tissue release MMPs and angiogenic growth factor that stimulates new blood vessel formation causes adipogenesis.

Angiogenic microvessels contribute to adipogenesis by numerous mechanisms-

I. Vessels supply nutrients and oxygen to the resident adipocytes, which require for growth and maintenance of cells.

II. Supply of plasma enriched in growth factors and cytokines by the vessels, trigger growth and survival signals in adipocytes to maintain their physiological functions. They supply circulating stem cells that are capable of differentiating into preadipocytes, adipocytes and vascular cells.

III. Infiltration of monocytes and neutrophils into the adipose tissue by the vessels augment the high numbers of inflammatory cells that are detected in obese individuals.

IV. Activated endothelial cells in angiogenic vessels produce various growth factors and cytokines that communicate with adipocytes in a paracrine fashion to promote their growth and expansion.

V. They remove waste products from the adipose tissue.

VI. Recent studies show that adipose tissue vasculature consists of fenestrated microvessels play essential role in regulating local or systemic effects of adipokines.

VII. Adipokines produced by expanded adipose tissue cause endothelial dysfunction. Impaired vascular function of adipose tissue alters the functions of other organs, which lead the development of diabetes, cardiovascular diseases, cancer and so on.

1.5. Targeted drug delivery

Paul Ehrlich first introduced the concept of targeted drug delivery nearly a century ago as "magic bullets" which guide a drug directly to its target organ and prevents it from affecting the healthy parts of the body [21]. Targeted drug delivery sometimes called smart drug delivery [22]. During the last three decades there has been intense effort directed towards the development of drug delivery systems (DDS) for treatment of diseases. In a broader sense, DDS can be defined as a strategy to efficiently convey the drug to its therapeutical site of action by the appropriate choice of carrier, route, and target. The efficacy of the DDS is determined by the selection of these three crucial factors.

1.6. Advantages of drug delivery systems

For achieving the goal of drug targeting, use of a carrier system for delivering drugs to the body provides several opportunities. Some prospective advantages of DDS are[21, 23]:

- Maintenance of constant drug levels in the therapeutical range.
- Reduction of drug toxicity and fewer side effects when targeted to specific tissues or organs.
- Facilitation of administration - increases patient compliance.
- Protection from degradation of biologically active drug molecules like peptides and proteins during transport.
- Smaller amounts of drug and decrease in the number of dosages.

1.7. Methods of drug targeting

Several methods of drug delivery are available and employed in experimental and clinical settings [24, 25]:

a. Direct application of drugs: In this method, drug is directly delivered on to the affected organ or tissue.

b. Passive targeting: This method exploits the increase in permeability of vascular endothelium in regions of inflammation and tumors. Drug carriers within the size range of 10-500 nm can extravasate and accumulate in the interstitial space in the regions of enhanced permeability (enhanced permeation and retention effect) e.g., tumors. Since the maximum size of the carrier that can extravasate at a particular

site varies on case basis, the size of the drug carrier can be used to control the efficacy of the drug.

c. Active targeting: This is a more advanced approach in which the drug delivery carrier has specific affinity for the target. The drug molecule could either be coupled to the targeting moiety or could be encapsulated in a carrier, which in turn is coupled to the targeting vector. Examples of targeting moieties are antibodies and their fragments [26], lectins, proteins, peptides [27], lipoproteins [28], hormones, charged molecules, polysaccharides, and oligonucleotides [29].

1.8. Liposomes for drug delivery systems

Liposomes are composed of natural or synthetic phospholipid bilayers consisting of an aqueous core (**Figure 1.4**). Therefore, any drug can be delivered to the site of action because lipophilic drugs can be encapsulated in the lipid bilayer and the hydrophilic drugs can be loaded in the aqueous compartment of the liposome [30]. Liposomes attract the attention greatly due to their composition and significant effort was made in this research area stimulate their use as drug delivery systems. **Table 3.1** lists liposomal drugs approved for clinical application or currently undergoing clinical evaluation.

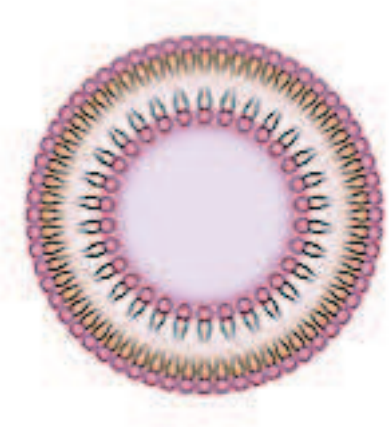

Figure 1.4: Liposomes are composed of phospholipid bilayer vesicles.

Table 1.2: Liposomal drugs approved for clinical application or undergoing clinical evaluation.

Active Drug	Product Name	Indication
Doxurubicin	Mycet	Comibined therapy of recurrent breast cancer
Doxurubicin in PEG-liposome	Doxil/ Caelyx	Breast cancer, ovarian cancer, refractory kaposis sarcoma
Vincristin	Onco TCS	Non- Hodgkin`s lymphoma
Amphotericin B	AmBisome	Fungal infection
Nystatin	Nyotran	Topical antifungal agent
Daunorubicin	DanoXome	Kaposi`s sarcoma
Annamycin	-	Doxorubicin-resistant tumors
Lurtotecan	NX211	Ovarian cancer

1.9. Aptamer

Aptamers are attractive class of targeting molecules, represented by short single-stranded oligonucleotides ligands. They are able to bind with high affinity and specificity to protein or non-protein targets by folding into complex secondary and tertiary structures [31, 32] (**Figure 1.5**).

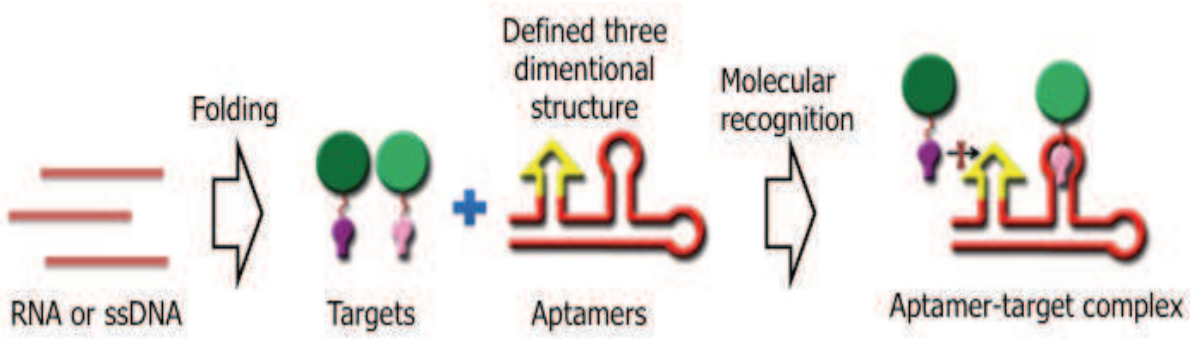

Figure 1.5: Secondary conformation and specific binding of aptamers to target.

They have ability to discriminate between closely related targets. Regarding these issues, aptamers are considered as alternative to antibodies for *in vivo* cell recognition. Owing to their relatively small size in comparison to antibodies, they are better suited for rapid target tissue penetration and blood clearance. These properties indicate a great potential of aptamers as targeting agents [33- 36].

1.10. SELEX

Aptamers are generated by an in vitro evolutionary selection, named SELEX (Systematic Evolution of Ligands by EXponential enrichment). Libraries contain random sequence oligonucleotides of large sequence complexity (generally between 10^{13} and 10^{15} members) [31, 32].

SELEX is an iterative process in which oligonucleotide libraries are incubated with the target of interest. The process is repeated until the pool is enriched for sequences that specifically recognize the target. The enriched pool is then cloned into bacteria, and positive clones are sequenced to obtain individual sequences. Still now, various selection modes have been developed, and each of these is rationally designed to suit the requirements of some specific purpose (37-43). One such modality is the implementation of cell-based aptamer selection, termed cell-SELEX [44- 49].

Cell-SELEX is the process where live cells are used to select aptamers for target recognition. This strategy motivated a promising selection approach for various applications because of the following reasons:

1. The molecular composition of the cell surface is not important in cell-SELEX.
2. The cell membrane surface is a complex system and has a countless number of molecules, especially proteins. In cell-SELEX, each of these molecules is used as potential target and a successful selection generate many ligands for different targets.
3. Cell-SELEX has the potential to develop aptamers for unknown molecules.

4. In cell-SELEX, aptamers bind to the native state of target molecules. So, the possibility of *in vivo* activity of aptamers is improved.

Thus, aptamers are very promising tools for cell-specific targeting and set out to enhance the toolbox of active targeting and drug delivering strategy.

Chapter 2

Aim and outline of this study

2

Aim and outline of this study

2.1. Aim of the study

Discovery of new drug compounds has stimulated the accelerated pace in recent years, with a considerable focus on the transition from *in vitro* to *in vivo* models. These require significant development of novel non-invasive, high resolution *in vivo* targeting approaches for studying disease development and quantitatively determining molecular and cellular events *in vivo* [50].

As discussed in introduction, obesity constitutes a key contributor to chronic disease, worldwide. Available treatments are insufficient to normalize body weight and prevent life-threatening complications. Therefore, effective drugs are urgently needed for the treatment of obesity and related disorders. Obesity or adipose tissue growth is highly correlated with angiogenesis. Thus, inhibition of angiogenesis might be a promising strategy to prevent growth of adipose tissue and ultimately the development of obesity.

Some non-specific angiogenesis inhibitors such as angiostatin [51], endostatin [52], TNP-470 [53, 54] and VEGFR2-specific inhibitors [55, 56] were able to prevent the development of obesity in high-fat diet mouse models. Due to lack of specific targeting some of these inhibitors produced toxicities to the healthy tissues.

To therapeutically target the adipose tissue vasculature, one possible approach is the delivery of drug utilizing a targeting motif that specifically binds to the vascular marker in the adipose tissue.

Considering this point, a peptide motif (CKGGRAKDC) specific to the vasculature in adipose tissue has been identified, using an *in vivo* phage display method. This motif specifically binds to the prohibitin receptor (a multifunctional membrane protein) expressed highly on the adipose vasculature [57]. Conjugation of this targeting peptide motif with an apoptosis-inducing peptide produced marked anti-obesity effects in mouse obesity models [57].

Recently, Hossen *et al*. have successfully developed an adipose vasculature-targeted nanocarrier referred to as prohibitin-targeted-nanoparticle (PTNP) utilizing the peptide ligand. This carrier can selectively accumulates into adipose tissue and successfully deliver drug molecules into the adipose endothelial cells. They have demonstrated the effective therapy for obesity in mice via a proapoptotic peptide/protein-loaded PTNP [58].

However, to date, no other targeting ligands to adipose vessels have been identified. Thus, in this study, to develop a novel adipose vasculature-targeted delivery system, we attempted to identify a nucleic acid aptamer, which can specifically recognize the adipose vascular endothelial cells, and to apply the identified aptamer as a ligand for targeted drug delivery system.

The ultimate objective of my work is-

I. Identification of novel nucleic acid aptamer of adipose ECs.

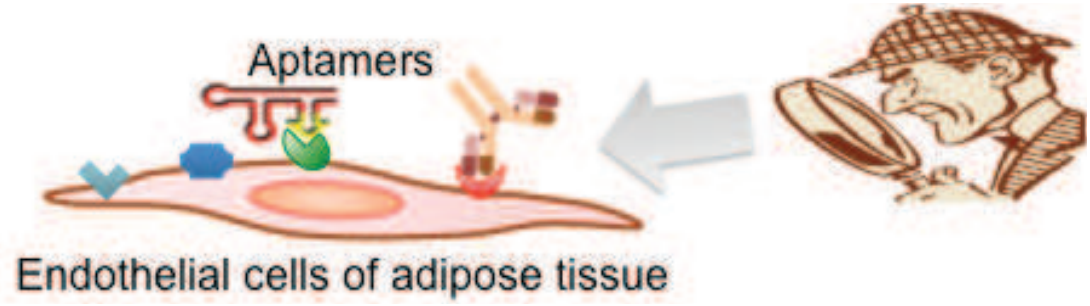

Figure 2.1: Schematic illustration of aptamer identification.

II. Development of a new drug delivery system modified by identified high affinity aptamers to adipose vessels.

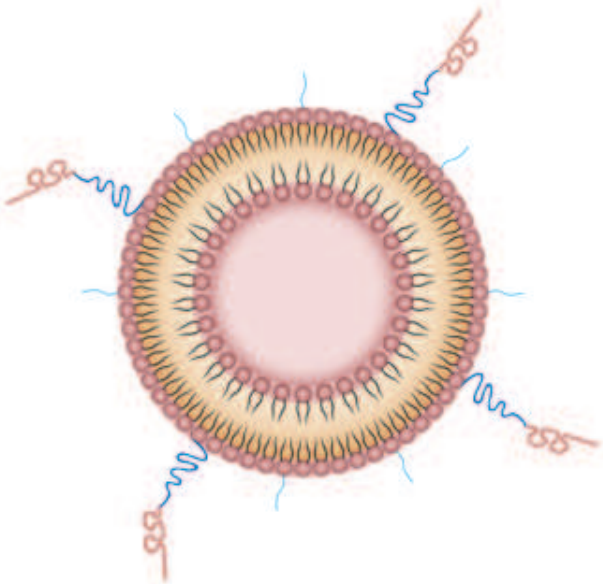

Figure 2.2: Schematic representation of aptamer-modified drug delivery system.

2.2. Outline of this dissertation

The aim of the work presented in this thesis was the identification of strong, novel nucleic acid aptamers of adipose endothelial cells and to develop novel drug delivery system utilizing the identified aptamers targeted to adipose vessels for control of obesity.

First, we report on the identification of nucleic acid aptamers of adipose endothelial cells. We used the combination of cell-based SELEX and *in vivo* SELEX method for the first time to identify aptamers. The progress of selection was observed through flow cytometric analysis. This combined strategy revealed highly frequent aptamers that can able to bind with adipose ECs not only *in vitro*, but also *in vivo*. Cloning and sequencing were carried out after *in vivo* SELEX and highly frequent two aptamers are selected from identified aptamers. Then the binding capability of the selected aptamers was assessed both *in vitro* and *in vivo*. Finally, binding assay assessed the non-importance of the primer region.

Then focused on the development of novel targeted drug delivery system for adipose vessels using selected two aptamers. Aptamer-modified liposome was prepared based on the prototype targeted-nanocarrier (PTNP). Then their *in vitro* and *in vivo* study was carried out.

Finally, optimization of the aptamer-modified liposomal composition was performed for targeting to adipose vessels. This study was based on the effect of free PEG

(length and density) on the targeted-liposome surface to recognize the target. We qualitatively and quantitatively analyzed the accumulation of targeted liposomes to elucidate the best liposomal composition for targeting adipose tissue.

Chapter 3

Materials and method

3

Materials and method

3.1. Reagents and animals

Distearoyl-sn-glycero-3-phoshoethanolamine-N-[methoxy (polyethylene glycol)-2000 (PEG2000-DSPE), cholesterol (chol) and sulfo-rhodamine (rhodamine) were purchased from Avanti Polar Lipids, Inc. (Alabaster, AL). Egg yolk phosphatidylcholine (EPC), PEG_{5k}-DSPE and PEG_{2k}-DSPE with a functional maleimide (Mal) moiety at the terminal end of PEG: N-[(3-maleimide-1-oxopropyl) aminopropyl polyethylene glycolcarbamyl] distearoyl-sn-Glycero-3-phosphoethanolamine and PEG_{5k}-DSPE with a functional succinimide (NHS) moiety at the terminal end of PEG: 3-(N-succinimidyloxyglutaryl)aminopropyl, polyethyleneglycol-carbamyl distearoylphosphatidyl-ethanolamine were purchased from Nippon Oil and Fat Co. (Tokyo, Japan). Hoechst 33342 was purchased from Dojindo laboratories (Kumamoto, Japan).

Peptide (Pep: GKGGRAKDGGC-NH2, purity: 93.6%, theoretical MW: 1004.15) and were synthesized by Kurabo Industries, Osaka, Japan.

The DNA library, unlabeled and labeled PCR primers were purchased and purified by Integrated DNA Technologies (Coralville, IA). The magnetic beads, M-270 was purchased from Invitrogen. EBM-2 media and the kits were purchased from Lonza, Walkersville, MD, USA.

Six weeks old male C57BL/6 J mice (body weight ~ 20 g) were purchased from SLC Japan (Shizuoka, Japan). The mice were maintained under standard housing conditions (standard mouse cages with a 12 h light/12 h dark cycle at 23 °C). Animal experiments involved standard procedures approved by the institutional animal care and research advisory committee of Hokkaido University, Sapporo, Japan.

3.2. Primers and library

A library of single-strand DNA that contained 40-mer random sequence region flanked by two 18-mer PCR primer sequences (5`-ATACCAGCTTATTCAATT-40N-AGATAGTAAGTGCAATCT-3′) was used in selection. The sense and antisense strand of the primers were labeled at the 5′ end with FITC (5′-FITC-ATACCAGCTTATTCAATT-3′) and at the 3′ end with biotin (AGATTGCACTTACTATCT- biotin-3′) respectively. The importance of FITC was to monitor the progress of selection by flow cytometry. The presence of biotin was used to separate the sense and antisense strands after PCR by streptavidin-biotin interaction followed by alkaline denaturation. After denaturation, the FITC-sense strand was used for next round of selection.

3.3. Cell culture

For cell-based SELEX, we used primary cultured adipose ECs derived from

C57Bl/6J mice. PCEC-EWAT cells were isolated from the blood vessels of epididymal adipose tissue from 9 to 10 week old male mice and cultured in EGM-2MV media (Lonza, Walkersville, MD) supplemented with 10% FBS and 0.1 mg/ml kanamicin sulfate (Wako Purechemicals, Tokyo, Japan) as described previously [59]. The cells were seeded onto culture dishes coated with 1.5% gelatin (SIGMA) and 10 μg/ml of human fibronectin (Asahi Glass, Tokyo, Japan) under an atmosphere of 5% CO_2/ air at 37 °C. For regular cell cultures, we used 0.05% trypsin to dissociate the cells from the surface of the culture dish. However, during the flow cytometry analysis, we used cell-detaching buffer to dissociate cells from the dish.

3.4. Cell-based SELEX method

Aptamer selection for adipose ECs was carried out on cultured dish without detaching cells from cultured dish. Before start of selection, the ssDNA library was first dissolved in EBM-2 media (100 μl), and heated in a thermo-block at 95 °C for 5 min, and then cooled on ice-water for 10 min to form secondary structures necessary for binding with the target cell surface protein. Then the volume of the library was adjusted up to 1ml with the binding media (EGM-2MV media free from FBS and antibiotics) for using in selections.

At first, the cells (1×10^6-2.5×10^5 cells from 1st to 9th round selections, respectively) on the cultured dish were washed with ice-cold HBSS to remove the dead cells. Then the snap-cooled ssDNA library (1nmol/ml in 1st round and 100pmol/ml from 2nd to 9th round selections) was applied on the cells and incubated on ice for 30 min.

The unbound libraries were then removed by aspiration. 3-5 times washing was performed with ice-cold binding buffer and HBSS to wash out the weakly bound DNA.

To collect bound DNA from cells, 500 µl of DNAse-free water was added to the washed cells, detached cells using cell scraper and transferred them into a 1.5 ml tube. Then heated the cell suspension at 95 °C for 10 min and recovered the DNA (supernatant) by centrifugation at 15,000 rpm for 10 min.

The bound DNA was purified by phenol-chloroform extraction followed by ethanol precipitation. For the phenol chloroform extraction, we added 500 µL of phenol-chloroform-isoamyl alcohols to 500 µL of bound DNA. After mixing well, the sample was centrifuged at 15,000 rpm for 10 minutes, and the supernatant was collected as the product. We performed the same extraction with fresh chloroform.

To prepare ssDNA library for the next selection round, we optimized the PCR conditions and amplified the isolated library by PCR. We performed total of 9th rounds of selections against only target cells.

PCR composition: (for 50 µl)

Water	34 µl
10X buffer with MgCl2	5 µl
2.5mM dNTPs	4 µl
FITC-forward primer	0.5 µl (1 µM)
Biotin-reverse primer	0.5 µl (1 µlM
Template (PCR1 product)	5 µl
Taq polymerase	0.5 µl

PCR condition:

Step	Temperature (°C)	Time (min)
Hot start	94	5
Denaturation	94	0.3
Annealing	50	0.3
Extension	72	0.3
Final extension	72	5
Hold	4	∝

3.5. *In vivo* counter SELEX

After 9th rounds of positive selections, we performed *in vivo* negative selection to remove the aptamers having binding affinity to ECs of other organs. For the negative selection, we injected 9th round of libraries (0.11nmol/kg body weight) to the vein of male C57Bl/6J mice and collected adipose tissue after 30 min of injection. The bound libraries were then recovered from tissue by heating the finely chopped adipose tissue in hot water (800 µl) at 95°C for 10min. Then the DNA (supernatant) was collected following centrifugation at 15,000 rpm for 10 min at 4°C and purified by phenol-chloroform extraction.

3.6. Aptamer binding assay by fluorescence activated cell-sorting analysis (FACS Analysis)

To estimate the extent of enrichment of binding of the ssDNA libraries as well as to produce a high affinity DNA aptamer, at first, selected libraries was dissolved in EBM-2 media and heated in a thermo-block at 95 °C for 5 min, and then cooled on ice- water for 10 min to form secondary structures. It should be noted here, that detached cells using cell-detaching buffer to avoid damage the cell surface proteins caused by using trypsin. 5×10^5 cells (50 µl) were incubated with FITC-ssDNA in 100 µl binding buffer containing 10% FBS for 30 min at 4 °C in dark condition.

To remove unbound DNA, washing was performed with binding buffer. Finally, the cells were suspended in MACS buffer (500 µl) and analyzed using FACS caliber

flow cytometer.

3.7. Cloning and sequencing of 10th round selected library

A small amount of DNA (250 pg) was amplified with unlabeled primers, purified and cloned into chemically competent E. coli using the TOPO TA Cloning Kit (Invitrogen). The transformed bacteria were plated out and grown overnight at 37°C. Bacterial colonies were then sent for sequencing. To determine the individual sequence for the selected colonies, we performed sequencing experiments based on the Sanger method by using a Big Dye Kit. An ABI prism 3130-AVANT Genetic analyzer was used to complete the sequencing analysis.

3. 8. Binding affinity of the aptamers

To determine the binding affinity of Seq1-full, Seq2-full, Seq1-40 and Seq2-40 to the adipose ECs, the cells were seeded on 96 well plates at the density of 1×10^4 cells/well. After 24 h, cells were treated with varying concentrations (Seq1-full: 10 nM-1 μM, Seq2-full: 3 nM-500 nM, Seq1-40: 10nM-600 nM and Seq2-40: 3nM-500 nM) of the selected aptamer pool in 50 μL of selection buffer containing 10% FBS on ice for 30 min in the dark. The cells were washed two times with selection buffer to wash out unbound aptamers. The cells were then lysed with the 1×lysis buffer and measured the fluorescent intensity of the bound aptamers using a fluorescence photometer. The mean fluorescence intensity of the target cells bound

to the aptamer was used to calculate the specific binding. The equilibrium dissociation constant Kd was determined by fitting the dependence of the fluorescence intensity of specific binding on the concentration of the ligands to the equation Y = Bmax X/(Kd+X) using the SigmaPlot 12 (Systat Software Inc., USA).

3. 9. Synthesis of Avecmer- PEG_{5k}-lipid

For the synthesis of Avecmer- PEG_{5k}-lipid, Avecmer-NH_2 and NHS-PEG_{5k}-DSPE were dissolved in distilled water separately. For the complete dissolution of NHS-PEG_{5k}-DSPE bath sonication was used. Avecmer-PEG_{5k}-DSPE was prepared by incubating a 1:1 (molar ratio) mixture of the NHS-PEG_{5k}-DSPE solution (10 mM) and the Avecmer (100 μM) for 24 h at 30 °C with continuous shaking on a Bio-shaker.

3. 10. Nanocarrier preparation and characterization

The Avecmer1-liposome, Avecmer2-liposome were prepared by following procedures-

3.10.1. Preparation of PEG_{2k}- liposome

PEG_{2k}-liposome was prepared by the REV (reverse phase evaporation) method [60]. For the preparation of this liposome, lipid containing EPC and cholesterol at a ratio of 2:1 (total lipid content: 5 μmol) separately dissolved in chloroform and Mal-PEG_{2k}-DSPE (for surface modification) was dissolved in distilled water. 5 μl of PEG_{2k}- DSPE (1 mol% of total lipid), 500 μl of 10 mM HEPES buffer (pH 7.4) and

500 µl of lipid solution were mixed and the solution was sonicated with a probe-type sonicator for 15 s at 4 °C. To prepare fluorescent labeled liposome, we used 0.5 mM rhodamine in 10 mM HEPES. The mixture was evaporated under a stream of N_2 gas followed by sonication for 1 min with a bath-type sonicator. For the removal of free rhodamine, ultracentrifugation was carried out two times for 30 min at 85,000 ×g in each wash.

3.10.2. Preparation of Avecmer- liposome

For the preparation of Avecmer-liposome, 0.625 mol% (of total lipid) of Avecmer-PEG_{5k}-DSPE was incubated with PEG_{2k}-liposome for 30 min at 37 °C with continuous shaking on a Bio-shaker. For the removal of free rhodamine after incubation, ultracentrifugation was carried out for 30 min at 85,000 ×g.

Pep- liposome and PEG- liposome was prepared by same method utilizing 0.625 mol% of Pep- PEG_{5k}- DSPE and Mal- PEG_{5k}- DSPE, respectively.

The size and zeta potential of the liposomes were determined by Malvern Zetasizer (Malvern instruments, Malvern, UK). The resulting liposomes were stored at 4 °C and used within 3 h of preparation.

3. 11. Cellular uptake study

Adipose ECs cells were seeded on sterile 35 mm glass-base dishes in the presence of their respective media described above. The cell density was 2×10^5 cells/well. The cells were incubated for 24 h to 50% confluence and then incubated with rhodamine loaded liposomes (Avecmer1-liposome, Avecmer2-liposome, Pep-liposome and PEG-liposome) (rhodamine dose: 0.2 µmol/ml) in a serum free medium for 3 h at 37

°C under an atmosphere with 5% CO_2. After incubation, the cell nuclei were stained with Hoechst 33342 (final concentration: 2.5 μg/ml) for 30 min and then washing was performed with medium, followed by heparin (20 U/ml) in 5 mM HEPES to remove the surface bound liposomes. After the washing procedures, 5 mM HEPES buffer supplemented with KCl 5.4 mM, $MgCl_2.6H_2O$ 1 mM, $CaCl_2.2H_2O$ 1.8 mM, and NaCl 138 mM, pH 7.3 was added and the cells were observed by confocal laser scanning microscopy by means of an oil- immersion objective lens (plan-apochromat x 63/NA (Carl Zeiss Co. Ltd., Jene, Germany).

3. 12. Homing of nanoparticles to blood vessels

The homing of liposomes in living adipose tissue was performed as described in the previous report [61] with minor modifications. For this study, male C57BL/6 J mice (6-week-old) were intravenously injected with rhodamine-loaded liposomes (Avecmer1-liposome, Avecmer2-liposome, Pep-liposome and PEG-liposome), at a rhodamine dosage of 0.2 μmol/kg. The recovery ratio of rhodamine (2.8 ± 0.5%) encapsulated into nanoparticles was taken into account in the dose calculation. For the visualization of blood vessels, FITC-Griffonia simplicifolia isolectin (GSIB4) was injected intravenously (50 μg/mice) 30 min prior to tissue collection. To collect tissues, mice were anesthetized and removed blood as much as possible by cardiac puncture. Tissues from the adipose epididymal regions, liver, and spleen were collected and washed 3 times with Hank's Buffered Salt Solution (HBSS) and then cut into small pieces (around 2 to 3 mm). After washing with HBSS, the pieces were transferred to light-protected disposable tubes containing PBS (pH 7.4) and then

placed on ice until used. The tissue pieces were then transferred to glass-based dishes and observed by confocal laser scanning microscopy (CLSM) (LSM-510; Carl Zeiss, or A1; Nikon). All images were recorded with sequential gaining of the fluorescent channels.

3.13. Liposome preparation and characterization for optimization

3.13.1. The selected six types of liposome were prepared by following two steps-

For the optimization of liposomal composition, EPC and chol at a ratio of 2:1 separately dissolved in chloroform, Mal- PEG_{2k}-DSPE and Mal- PEG_{5k}-DSPE was dissolved in distilled water. 1mol% PEG_{2k}-liposome, 2.5mol% PEG_{2k}-liposome, 5mol% PEG_{2k}-liposome, 1mol% PEG_{5k}-liposome, 2.5mol% PEG_{5k}-liposome and 5mol% PEG_{5k}-liposome were prepared by the incorporation of Mal- PEG_{2k}-DSPE and Mal- PEG_{5k}-DSPE with the density of 1mol%, 2.5 mol% and 5 mol% of total lipid respectively.

To prepare fluorescent labeled liposome, we used 0.5 mM rhodamine in 10 mM HEPES. For the removal of free rhodamine, ultracentrifugation was carried out two times for 30 min at 85,000 ×g.

3.13.2. Avecmer- PEG_{5k}-DSPE was attached on the surface of these six types of liposomes at a density: 0.625 mol% of total lipid. Condition for the incubation was 30min at 37°C with continuous shaking on a Bio-shaker. After incubation,

ultracentrifugation was carried out for 30 min at 85,000×g to remove free rhodamine.

The size and zeta potential of the liposomes were measured by Malvern Zetasizer (Malvern instruments, Malvern, UK). The resulting liposomes were stored at 4 °C and used within 3 h of preparation.

3.14. Comparative targeting of optimized liposomes to adipose vasculature

For the comparative study of the six liposomes, male C57BL/6 J mice (6-week-old) were intravenously injected with rhodamine-loaded liposomes (1 mol% PEG_{2k}-liposome, 2.5 mol% PEG_{2k}-liposome, 5 mol% PEG_{2k}-liposome, 1 mol% PEG_{5k}-liposome, 2.5 mol% PEG_{5k}-liposome and 5 mol% PEG_{5k}-liposome), at a rhodamine dosage of 0.13 μmol/kg. The Recovery Ratio of rhodamine (2.8 ± 0.5%) encapsulated into nanoparticles was taken into account in the dose calculation. FITC-Griffonia simplicifolia isolectin (GSIB4) was injected intravenously (50 μg/mice) 30 min prior to tissue collection for the visualization of blood vessels. To collect adipose tissues, mice were anesthetized and blood was removed by cardiac puncture as much as possible. Tissues from the adipose epididymal regions were collected and washed 3 times with Hank's Buffered Salt Solution (HBSS) and then cut into small pieces. After washing with HBSS, the pieces were transferred to light-protected disposable tubes containing PBS (pH 7.4) and then placed on ice until used. The tissue pieces were then transferred to glass-based dishes and observed by

confocal laser scanning microscopy (CLSM) (LSM-510; Carl Zeiss, or A1; Nikon). All images were recorded with sequential gaining of the fluorescent channels.

3.15. Quantitative measurement of nanoparticles accumulated in tissues

Male C57BL/6J mice (6-week-old) were intravenously injected with rhodamine-loaded liposomes. For the visualization of blood vessels, FITC-Griffonia simplicifolia isolectin (GSIB4) was injected intravenously (50 μg/mice) 30 min prior to tissue collection and adipose tissue was observed by CLSM. All images were exported as 8-bit TIFF-format image data and then transferred to the Image-J software (Media Cybernetics Inc., Silver Spring, MD). All of the stack files used as merged files was used to measure pixel area count, which satisfy the threshold pixel intensity in each RGB images or an arbitrary combination of RGB channels in a selected region. Digital noise was nullified by single pixel signals.

Chapter 4

Results

4
Results

4.1. Cell-SELEX for enrichment of aptamer candidates for target cells

Aiming for DNA aptamers binding to adipose ECs, we used cell-based SELEX method during the *in vitro* selection experiment. Selection was carried out on culture dish to maintain the native state of target molecules on cell surface. Primary cultured murine adipose ECs was used as the target for aptamer selection.

In our selection, a library of ssDNAs that contained 40-mer random sequence region flanked by two 18-mer PCR primer sequences was used. In 1st round selection, ssDNA library of 1nmol was incubated with the target cells to allow binding to take place. The cells were then washed, and the DNA sequences bound to the cell surface were eluted (**Figure 4.1**). The collected sequences were then amplified for the next-round selection (**Figure 4.2**). During cell-SELEX, the selection conditions and library amount were gradually changed with the progress of selection rounds. After multiround selection, the subtraction process efficiently enriched the target-cell aptamer candidates.

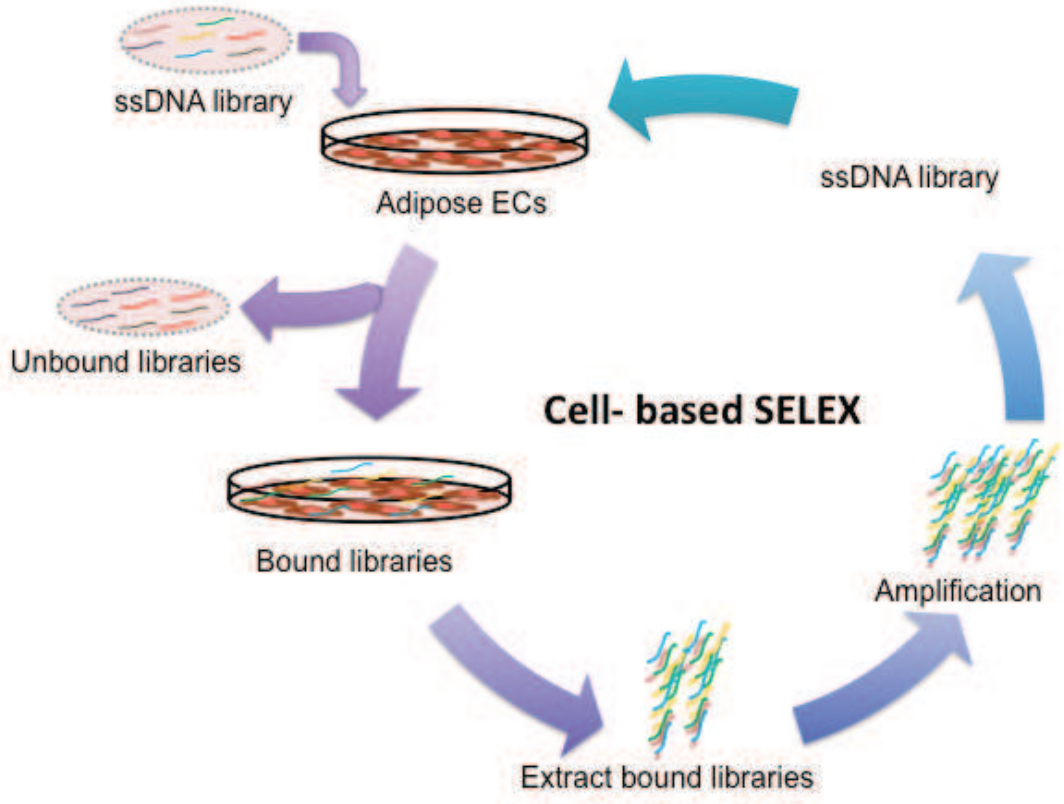

Figure 4.1: A schematic representation of the cell-based SELEX method used for the selection of DNA aptamer. ssDNA library was incubated with adipose ECs on ice for 30 minutes. After incubation, unbound DNA was removed. Bound ssDNA from cells were collected and eluted by heating at 95 °C for 5 minutes. Extracted ssDNA pools were subjected to amplify with fluorescent tag to start the next cycle.

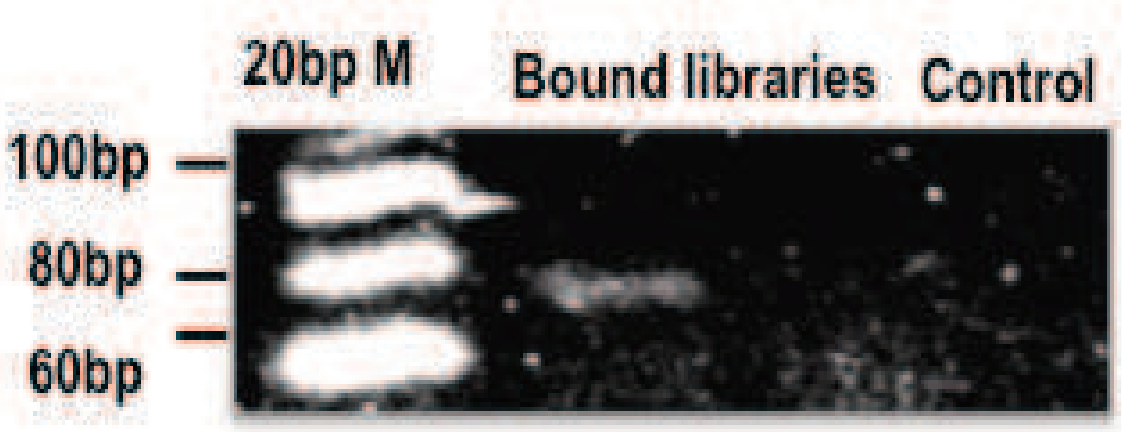

Figure 4.2: Agarose gel electrophoresis of amplified DNA. After 1st round selection, the extracted ssDNA was amplified and subjected on 3.8 % agarose gel for electrophoresis. To observe the DNA band, the gel was stained with etidium bromide.

In addition, flow cytometry analysis (FACS) was carried out to monitor the progress of selection process. DNA library collected after selections were labeled with FITC dye and incubated with live cells. After incubation, the fluorescence intensity of the labeled cells was measured by the flow cytometry analysis.

After 1st round SELEX, the binding of isolated DNA library to adipose ECs was assessed by flow cytometry (**Figure 4.3 a ~ f**). As shown in **Figure 4.3 (a)**, the fluorescence intensity of adipose ECs was slightly increased by treatment with the 1st round library. This indicates that the recovered DNA molecules having the binding ability to adipose ECs. Thus, the process was carried out repeatedly. FACS data represented the progress of bound DNA to target cells with the increment of selection cycles (**Figure 4.3**). Moreover, the saturation of cell-SELEX was achieved after 9th cycle selection, confirmed from the merged fluorescence intensity of bound DNA between 8th and 9th cycle (**Figure 4.3 (f)**).

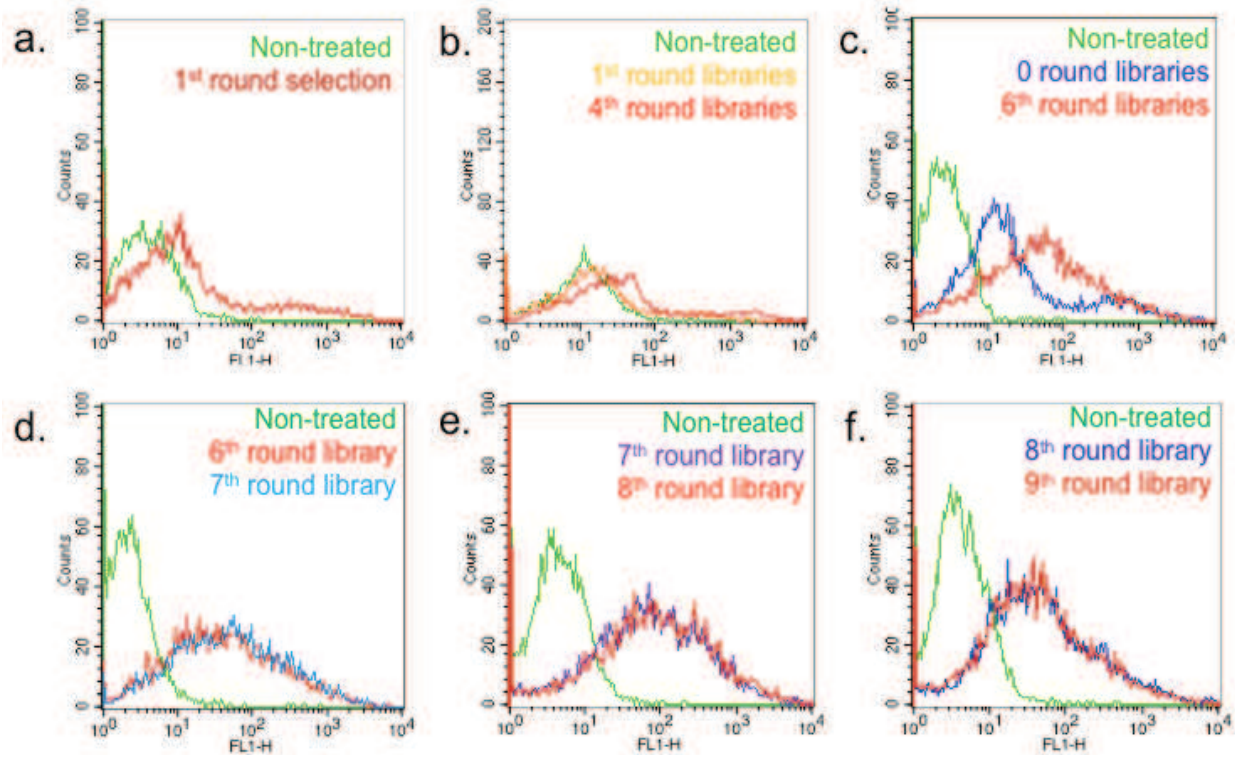

Figure 4.3: Flow cytometry binding assay of selected FITC labeled ssDNA pools with adipose ECs. Enrichment in binding random ssDNA in the selection was observed by flow cytometry analysis. 100 pmol of ssDNA library was used in each case. (**a-c**) Fluorescence intensity of bound aptamers increases with the increase of selection rounds, (**c**) zero-round ssDNA pool was used to observe the differentiation of enrichment from the starting point of selection with 6th round selection, (**d-e**) After 6th round SELEX difference of intensity shift was not observed.

After saturation of targeted aptamers in cell-SELEX, it was necessary to eliminate the undesired aptamers candidates, which had possibility to bind to endothelial cells of other organs in the body, and we also wanted to confirm the binding ability of enriched aptamers *in vivo*. Thus, we followed *in vivo* aptamer selection (10^{th} cycle selection) by intravenous injection of the 9^{th} round DNA library to mice. After 30 min of injection, adipose tissue was collected; bound DNA was extracted and amplified (**Figure 4.4**). Strong band appeared in polyacrylamide gel electrophoresis confirmed the successful isolation of aptamer candidates from *in vivo* counter selection (**Figure 4.5**).

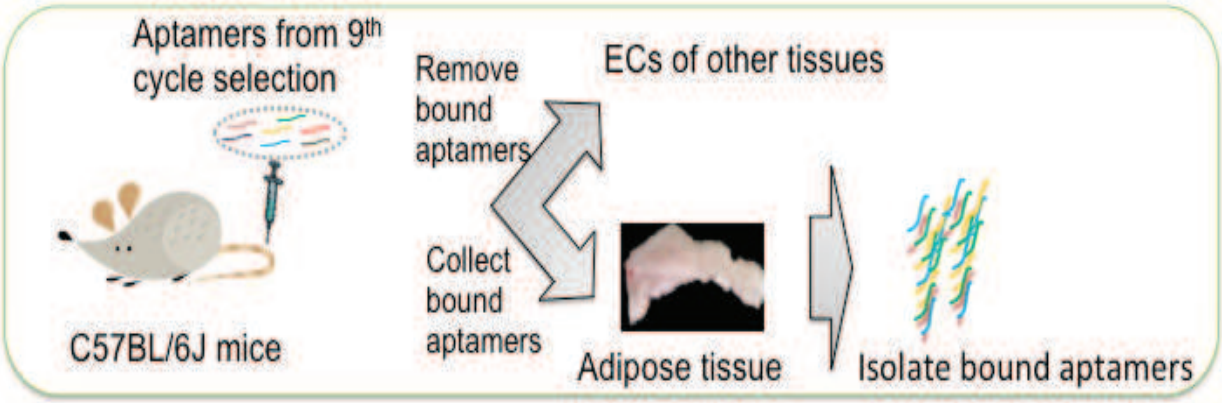

Figure 4.4: *In vivo* counter selection (10^{th} round SELEX). 9^{th} round ssDNA was i.v.-injected to mice. Adipose tissue was collected prior to 30 min of injection. The bound library was then extracted from adipose tissue.

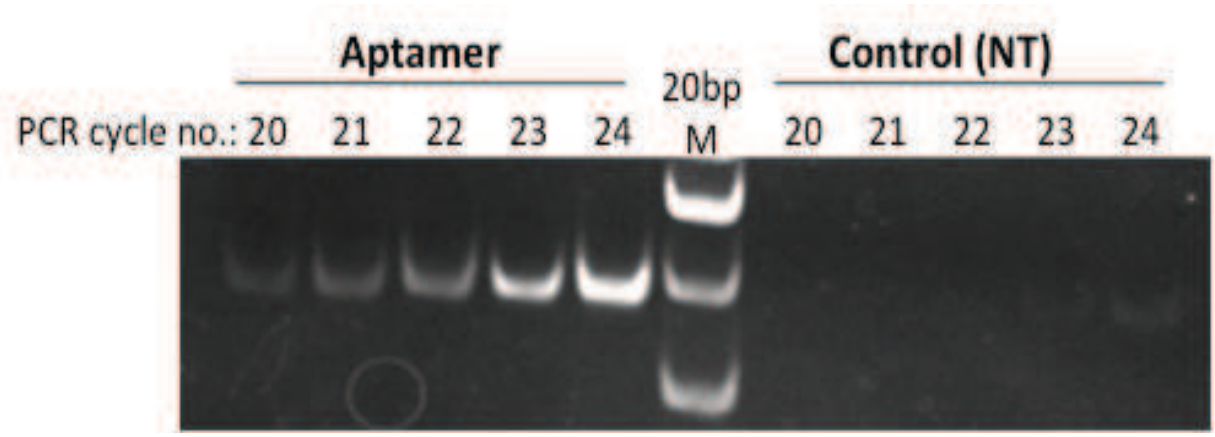

Figure 4.5: Confirmation of isolated aptamers from adipose tissue after *in vivo* SELEX. After 30 min i.v.- injection of 9th round aptamers, the bound ssDNA was extracted, amplified and subjected to 8% polyacrylamide gel electrophoresis. To observe the DNA band, the gel was stained with etidium bromide.

4.2. Identification of aptamers for the target cells

After isolation of *in vivo* aptamers, the random ssDNA pools that bound to adipose ECs with high affinity were used in cloning experiments, using a TOPO-TA cloning kit (Invitrogen) followed by sequencing using the Sanger method via a sequencer, to identify the sequences of individual aptamer candidates (**Figure 4.6**). The sequences were assembled based on the homology of the DNA sequences of individual clones with each group containing very similar sequences.

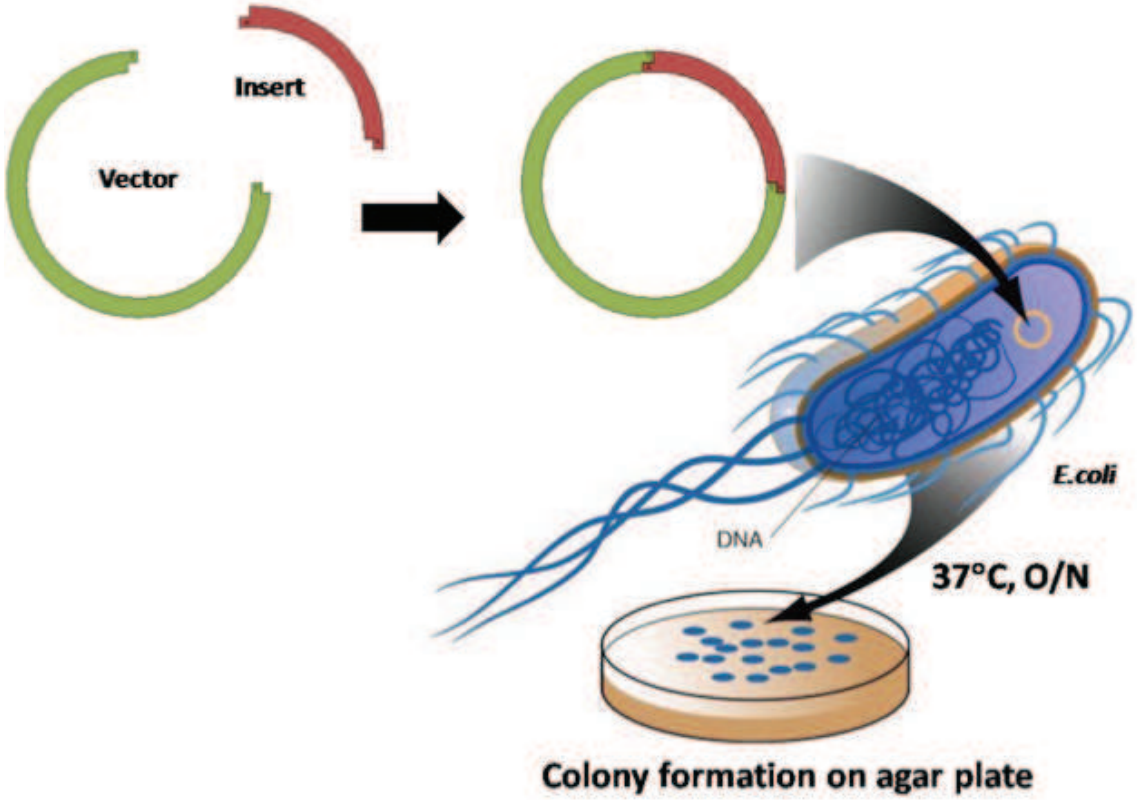

Figure 4.6: Cloning of 10th round selected library. Unlabelled ssDNA was incorporated into the TOPO cloning vector and inserted into *E.coli*. Transformed *E.coli* subjected on agar plate and incubated over night 37 °C.

Among 92 clones, two sequences were selected due to the presence of high frequencies (31 and 21) and named as Seq1 and Seq2 (**Table 4.1**).

Table 4.1: Sequences of identified aptamers

Sequence	Frequency
Seq1	31/92
Seq2	21/92
Seq3	5/92
Seq4	5/92
Seq5	2/92
Seq6	2/92
Seq7	2/92
Seq8	2/92
Seq9	1/92
Seq10	1/92
Seq11	1/92
Seq12	1/92
Seq13	1/92
Seq14	1/92
Seq15	1/92
Seq16	1/92
Seq17	1/92
Seq18	1/92
Seq19	1/92
Seq20	1/92
Seq21	1/92
Seq22	1/92

4.3. Binding assay of the selected aptamers *in vitro* and *in vivo*

Although we performed *in vivo* counter selection against along with positive selection, it was very important to verify that the selected two aptamers actually binds to the target cells *in vitro* and *in vivo*.

For *in vitro*, a binding assay of Seq1 and Seq2 was performed with the primary cultured adipose ECs to evaluate its binding capacity by flow cytometry (**Figure 4.7**). To determine the binding affinity random library was taken as control. Fluorescence intensity shifts of both Seq1 and Seq2 exhibited higher binding capability compare to the random library (**Figure 4.7**). The high affinity binding of Seq1 and Seq2 have proved the possibilities of its binding capability to the target cell *in vitro*.

4.4. Assessment of selected aptamers to murin white vasculature

To assess the targeting capability of the selected aptamers to adipose vessel, Seq1 and Seq2 were injected to C57BL/6J mice from tail vein. At 30 min after injection, adipose tissue from mice was collected and extracted the DNA fraction from tissue. After PCR amplification, the samples were subjected to polyacrylamide gel electrophoresis (PAGE). The random (0 cycle) DNA library was used as a negative control. As a result, the strong 76 bp bands were appeared in both of Seq1 and Seq2 treated samples, compared to the control (**Figure 4.8**). Result revealed that both selected aptamers has ability to home in adipose vessel.

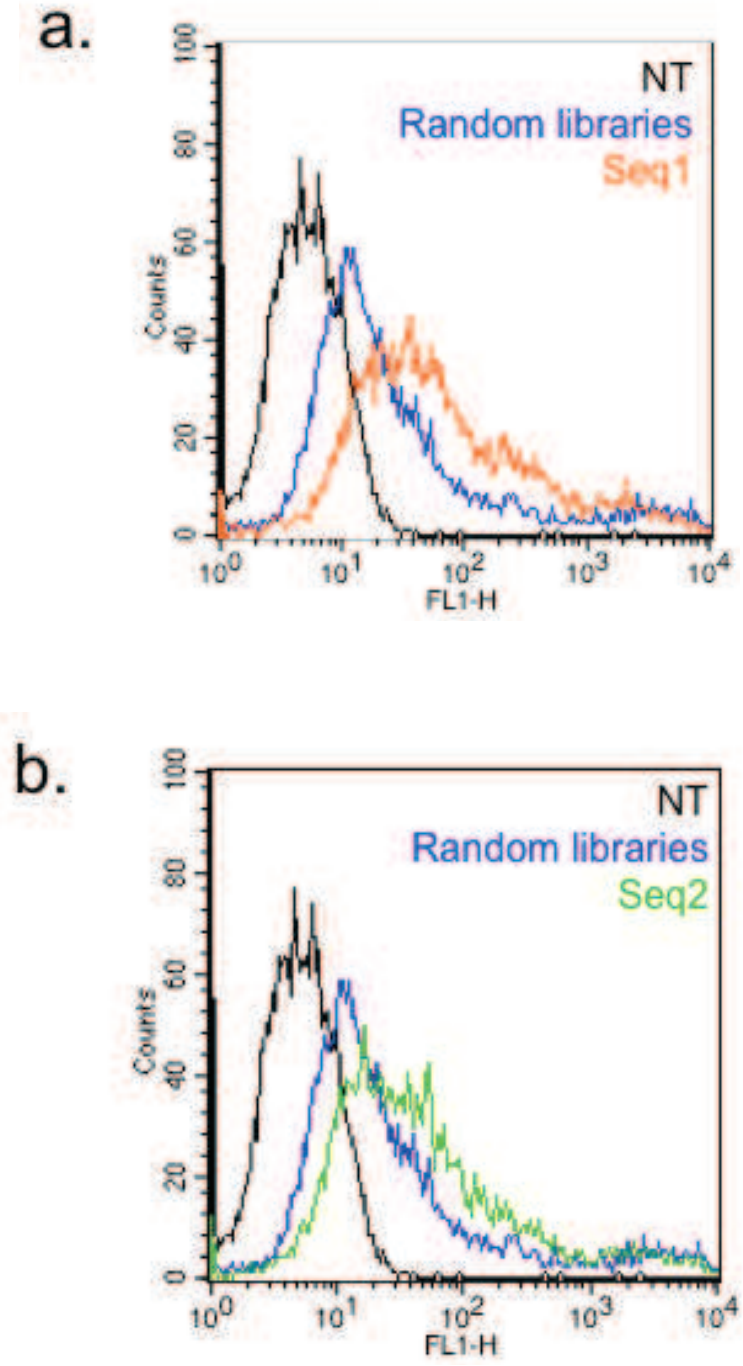

Figure 4.7: Binding assay of selected FITC-labeled DNA aptamer **a.** Seq1 and **b.** Seq2 against adipose ECs by flow cytometry assay. Random library was used for negative control. The amount of FITC- library was 100 pmol.

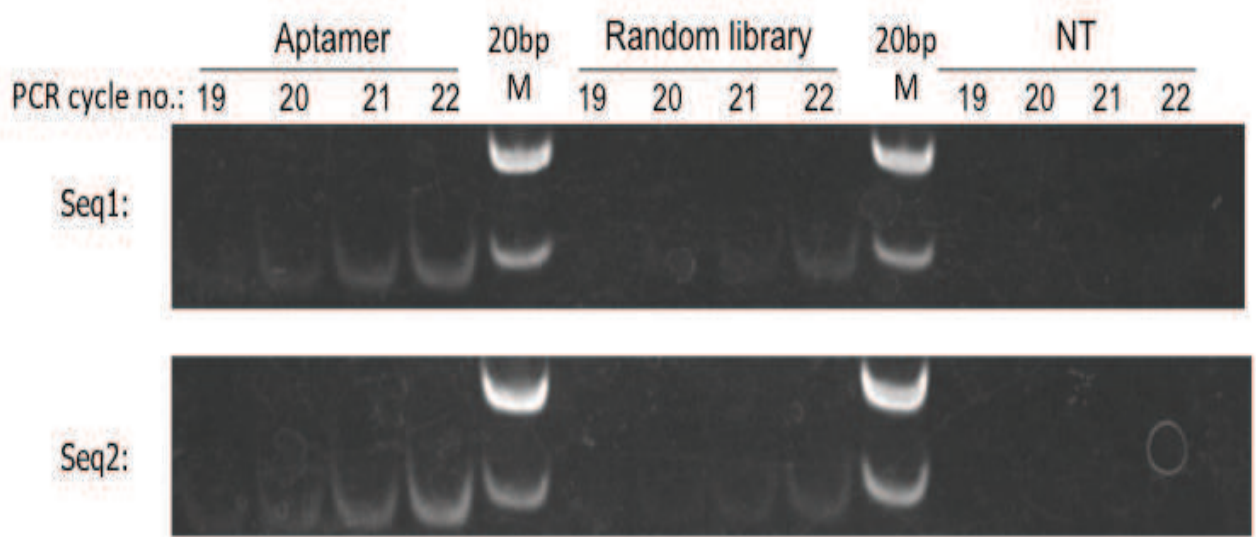

Figure 4.8: Homing of selected aptamers to adipose tissue *in vivo*. After 30 min i.v.-injection of Seq1 and Seq2, the bound ssDNA was extracted, amplified and subjected to 8% polyacrylamide gel electrophoresis. The gel was stained with etidium bromide to observe the DNA band.

4.5. Removal of primer regions from sequence

Generally, all nucleotides of a full-length aptamer (Random region edged by primer regions) are not responsible for target binding. The non-binding domain can affect the actual binding interaction between aptamer and target. So, truncation of selected sequences and identification of binding domains is very important step to find out the high affinity aptamers. Moreover, primer regions are not expected to interfere in secondary structure formation and target binding. But in several cases, primers interfere for target binding and structure formations.

In case of Seq1 and Seq2, primers were responsible for secondary structure formation. Thus, we wanted to confirm whether these regions are responsible for target binding or not. To confirm this issue, we examined the binding assay of central 40-mer bases (removing primer regions from both sides) and compared with full-length aptamers. Flow cytometric result expressed the similar binding pattern of Seq1-40 and Seq2-40 with full-length (76 mer) aptamers (**Figure 4.9).** Therefore, Seq1-40 and Seq2-40, rather than full-length (76 mer) aptamers, were used for the following experiments and they were termed as Avecmer (Adipose vascular endothelial cell-targeted aptamer) 1 and Avecmer 2, respectively.

The binding affinity of Seq1-full, Seq2-full, Seq1-40 and Seq2-40 to the adipose ECs (**Figure 4.10** (**a-d**)) also confirmed that primer regions were not responsible for target binding.

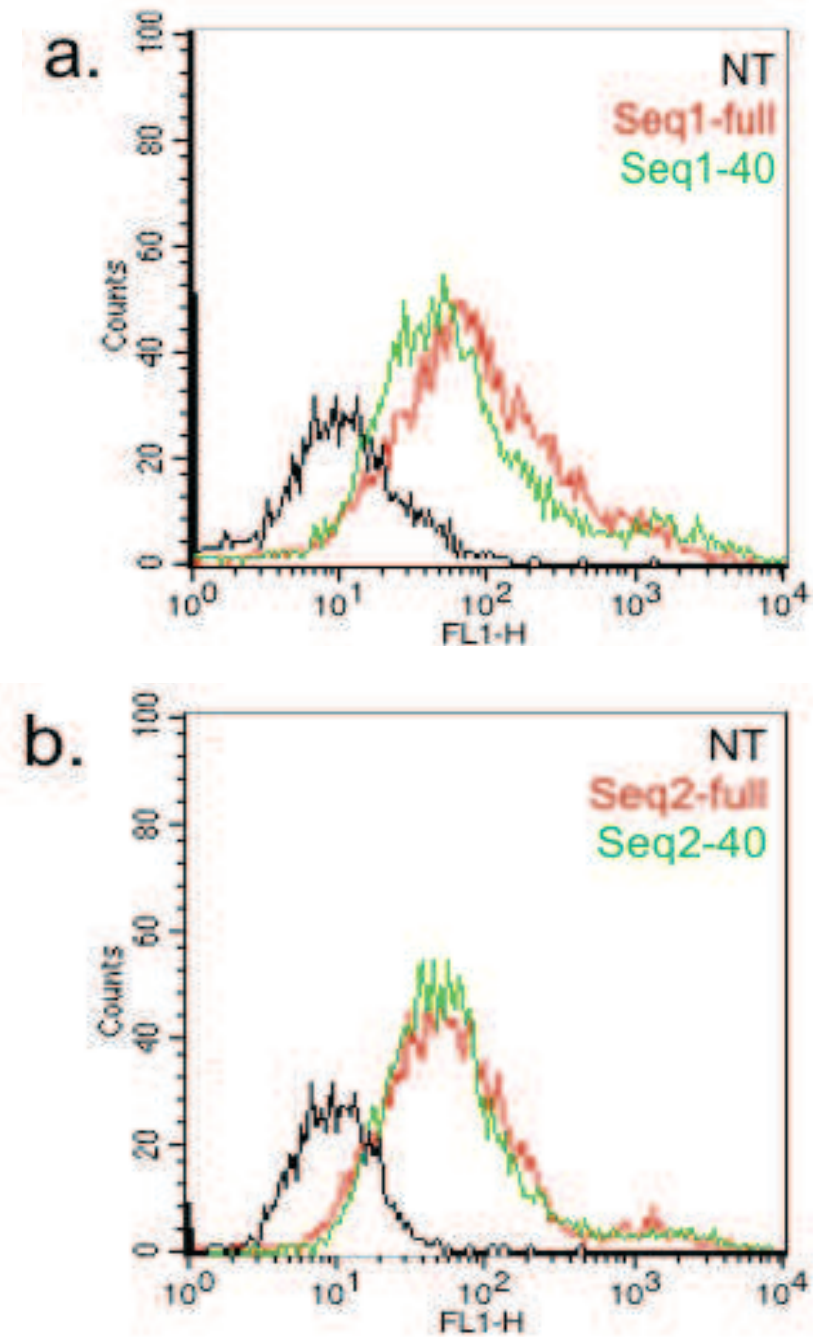

Figure 4.9: Flow cytometry histogram showing binding competition between the full length and 40 mer aptamers, **a.** Seq1 and **b.** Seq2. Red: full-length Seq, green: 40 mer Seq and black non-treated cells.

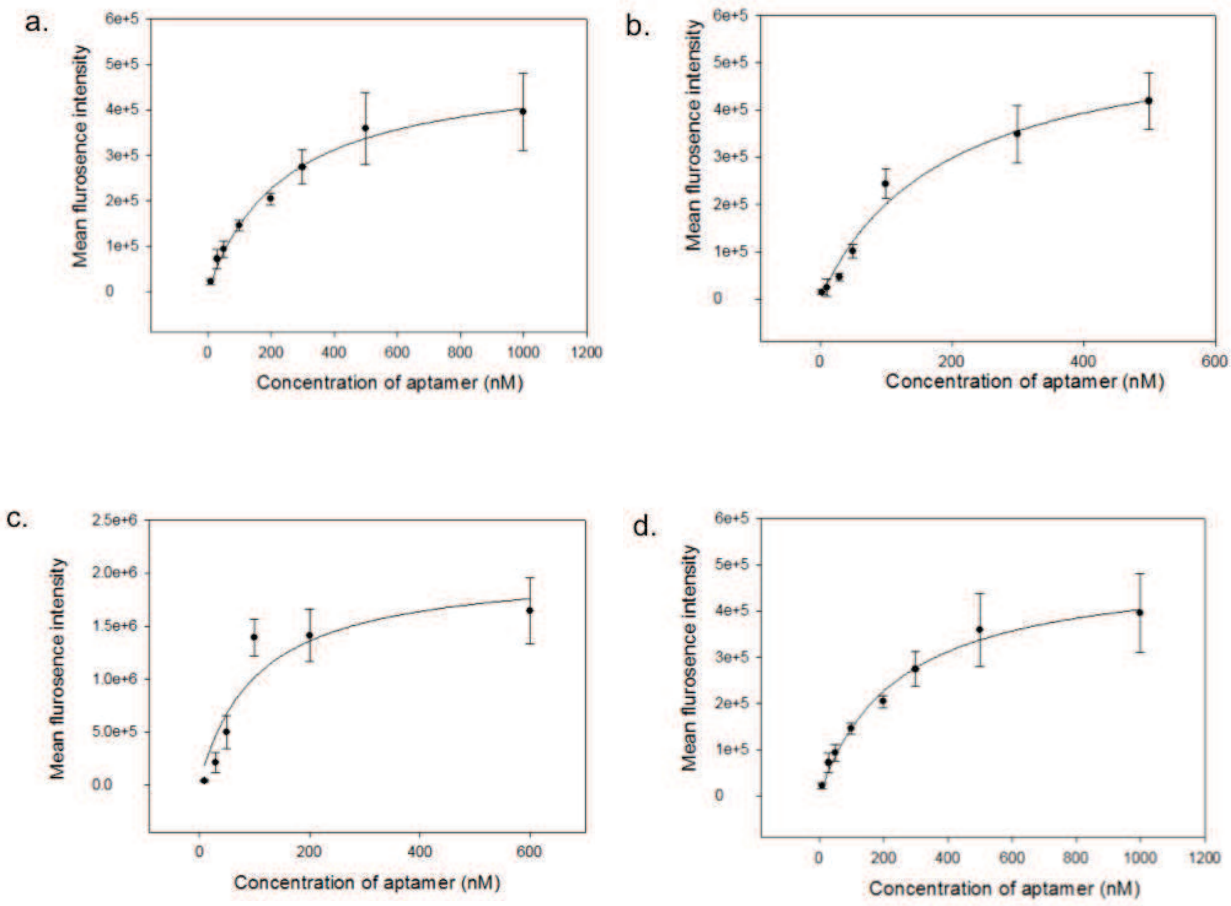

Figure 4.10: Determination of binding affinity, Kd value of the DNA aptamers. The Binding affinity of a. Seq1-full: 242.40 nM ± 32.9 nM, b. Seq2-full: 187.55 nM ± 51.45 nM, c. Seq1-40: 103.5 nM ± 54.75 nM and d. Seq2-40: 127.02 nM ± 30.67 nM were determined using FITC-labelled aptamers to adipose ECs. Data represent mean ± SD (n=3).

4.6. Physicochemical characterization of liposomes

In order to observe the applicability of Avecmer1 and Avecmer2 as active targeted drug delivery system, we prepared liposomes modified with these two selected aptamers. Here, Pep-liposome and PEG-liposome were also prepared as control. (**Figure 4.11**) After preparation, average particle size and charge of Avecmer1-liposome, Avecmer2-liposome, Pep-liposome and PEG-liposome were measured by Malvern Zetasizer. As shown in **Table 4.2**, the liposomes (Avecmer1-liposome, Avecmer2-liposome, PEG-liposome) had negative (−22.8 mV, -23.1 mV and -13.3 mV) and almost neutral (0.38 mV) zeta potentials, respectively. Due to the negative charge of nucleic acid aptamers and PEG_{5k}-DSPE, the Avecmer1-liposome, Avecmer2-liposome and PEG-liposome increased negativity and due to slight positive charge of the peptide, the peptide-modified liposomes neutralized the negativity of the liposome surface.

Table 4.2. Physicochemical property of liposomes

	Size (nm)	ζ-potential (mV)
Avecmer1-liposome	163.2	-22.8
Avecmer2-liposome	167.4	-23.1
Pep- liposome	189.7	0.38
PEG-liposome	157.6	-13.3

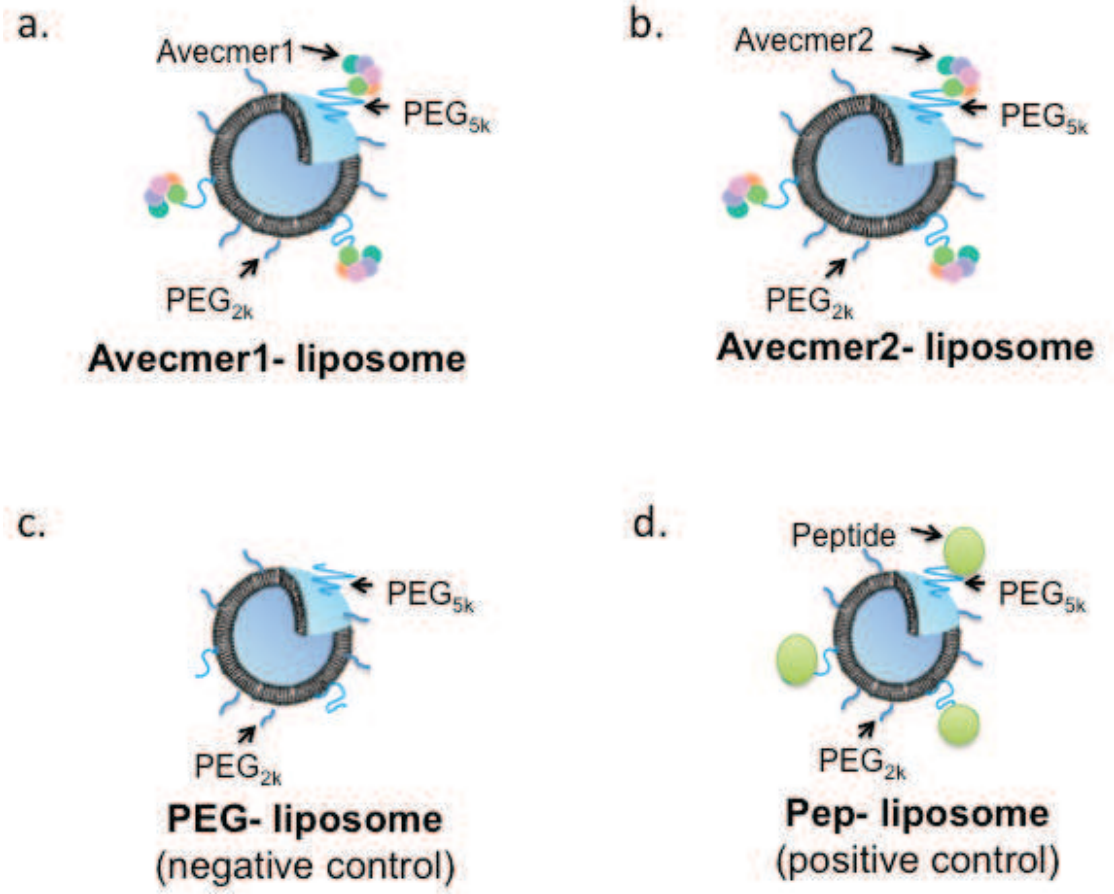

Figure 4.11: Preparation of Avecmer- modified liposomes. **a.** Avecmer1-liposome, **b.** Avecmer2-liposome, **c.** PEG-liposome and **d.** Pep-liposome.

4.7. Cellular uptake study of liposomes

For the evaluation of the feasibility of Avecmer1-liposome and Avecmer2-liposome as delivery vehicle, we analyzed whether the liposomes are being taken up by adipose ECs.

To achieve this, the rhodamine-loaded Avecmer1-liposome and Avecmer2-liposome were applied to target cells; Pep-liposome and PEG-liposome were utilized as positive and negative control, respectively. The cellular uptake of liposomes was observed by a confocal laser-scanning microscopy (CLSM). Both of Avecmer1-liposome and Avecmer2-liposome showed the higher internalization into adipose ECs, compared to PEG_{5k}-lip (negative control). But the internalizing capacity was lower than the Pep-liposome (**Figure 4.12**). These results demonstrated that nanoparticle modified with both Avecmer1 and Avecmer2 could be taken up into the adipose ECs but the uptake efficiency was lower than Pep-liposome.

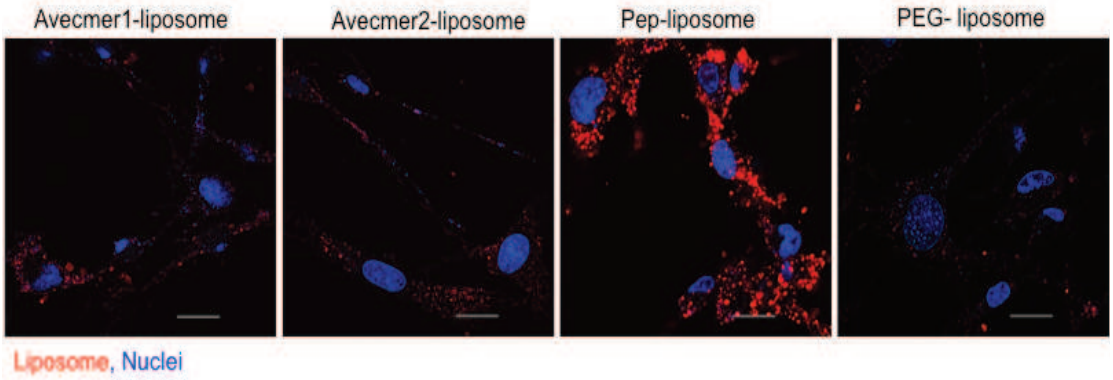

Figure 4.12: Cellular internalization of Avecmer1-liposome and Avecmer2-liposome to adipose ECs. Cells were incubated with rhodamine-loaded Avecmer1-liposome, Avecmer2-liposome, Pep-liposome and PEG-liposome for 3 h at 37 °C. Nuclei were stained with Hoechst 33342. Cells were observed by means of confocal laser scanning microscopy (CLSM). Scale bar indicated 100 μm.

4.8. *In vivo* selectivity of aptamer modified liposome

In vivo imaging is a powerful method, which reveals tissue distribution of dye-loaded particles during a period of time. To endorse the targeting effect *in vivo*, the feasibility of aptamer-modified liposome as an *in vivo* carrier was assessed. After i.v.-injection of rhodamine-loaded Avecmer1-liposome and Avecmer2-liposome to normal mice, the accumulation of the liposomes to adipose tissue, liver and spleen was observed by CLSM.

The clear fluorescence signal of Avecmer1-liposome and Avecmer2-liposome was appeared in the blood vessels of adipose tissue (**Figure 4.13**), whereas PEG_{5k}-lip (negative control) was not (**Figure 4.13)**. Moreover, the intensity signal of Avecmer1-liposome and Avecmer2-liposome was much more higher than Pep-liposome. These results exhibited that both Avecmer1 and Avecmer2 have the ability to home in adipose tissue greater than the peptide ligand (reverse result of *in vitro* study).

In addition, the accumulation of Avecmer1-liposome and Avecmer2-liposome was observed in liver and spleen. Both liposomes were detected in liver and spleen, however, the fluorescence intensity was similar with the PEG_{5k}-liposome and Pep-liposome (**Figure 4.14**). These results demonstrated that both aptamer-modified liposomes could efficiently target the adipose vessels.

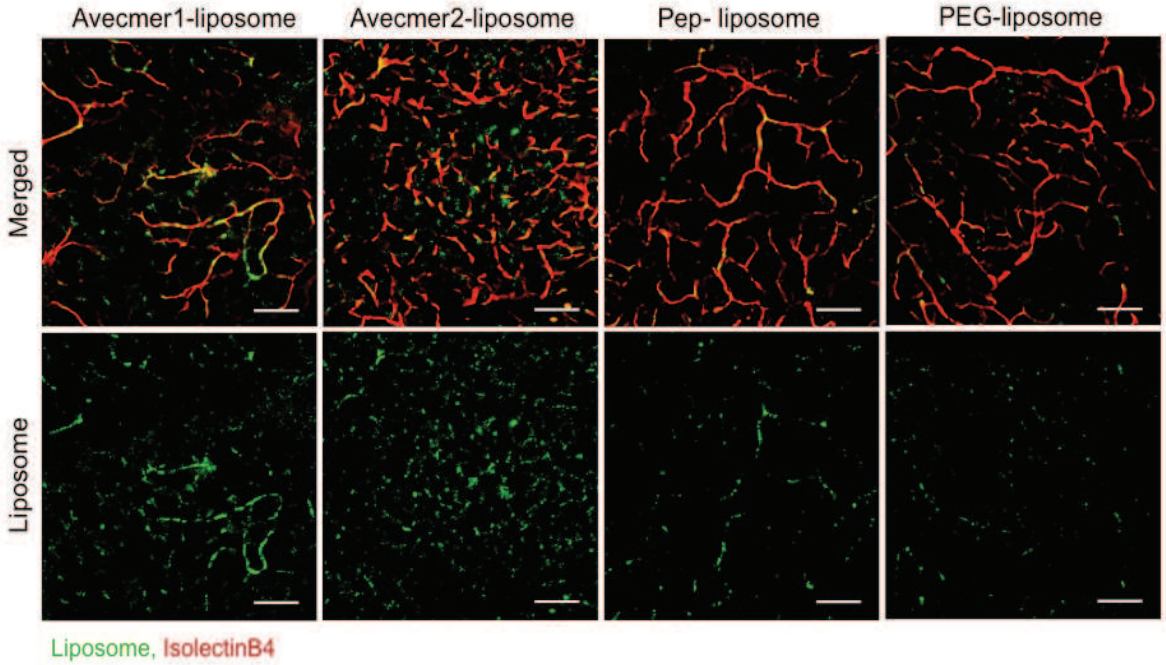

Figure 4.13: In vivo targeting ability of Avecmer1-liposome and Avecmer2-liposome to adipose vessels in normal mice. Mice were i.v.-injected with rhodamine-loaded Avecmer1-liposome, Avecmer2-liposome, Pep-liposome and PEG-liposome (green). To visualize blood vessels, 50 μg of FITC-GSIB4 (red) was also i.v.-injected 30 min prior to tissue processing. At 17 h after administration, adipose tissue was observed with CLSM. Scale bars represent 100 μm.

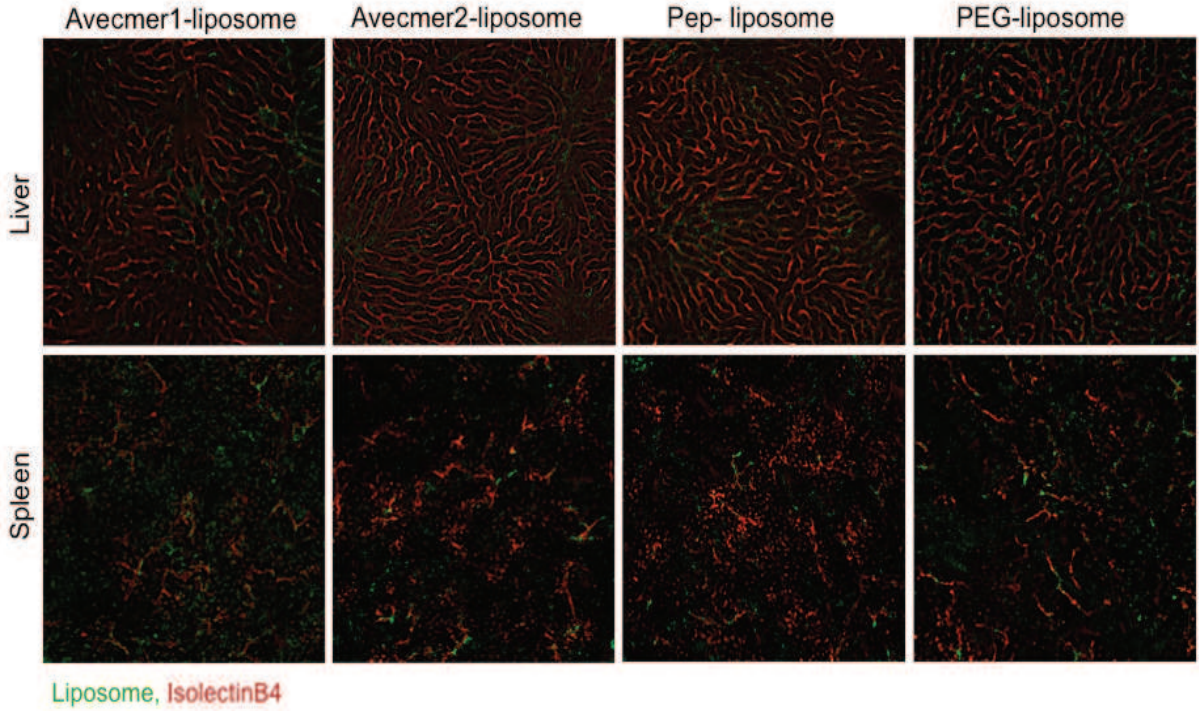

Figure 4.14: Accumulation of Avecmer1-liposome and Avecmer2-liposome to liver and spleen in normal mice. Mice were i.v.-injected with rhodamine-loaded Avecmer1-liposome, Avecmer2-liposome, Pep-liposome and PEG-liposome (green). For the visualization of blood vessels, 50 μg of FITC-GSIB4 (red) was also i.v.-injected 30 min prior to tissue processing. At 17 h after administration, tissues were observed with CLSM. Scale bars represented 100 μm .

4. 9. Physicochemical properties of liposomes

In order to optimize the liposomal composition for *in vivo* delivery, we prepared six types of liposomes (1 mol% PEG_{2k}-liposome, 2.5 mol% PEG_{2k}-liposome, 5 mol% PEG_{2k}-liposome, 1 mol% PEG_{5k}-liposome, 2.5 mol% PEG_{5k}-liposome and 5 mol% PEG_{5k}-liposome) modified with two selected aptamers (Avecmer1 and Avecmer2). Here, 1mol% of PEG_{2k}-liposome was taken as control (**Figure 4.15**). After preparation, average particle size and charge of all liposomes were measured by Malvern Zetasizer. Due to the negative charge of nucleic acid aptamers and PEG_{5k}-DSPE, the zeta potential of the liposomes were negative (**Table 4.3** and **Table 4.4**).

Table 4.3. Physicochemical property of Avecmer1-liposomes

Liposome	Size (nm)	ζ-potential (mV)
1mol% PEG_{2k}- liposome	151.3	-20.3
2.5mol% PEG_{2k}- liposome	136.7	-20.2
5mol% PEG_{2k}- liposome	122.2	-21.3
1mol% PEG_{5k}- liposome	130.9	-14.1
2.5mol% PEG_{5k}- liposome	122.7	-11.7
5mol% PEG_{5k}- liposome	118.8	-11.4

Table 4.4. Physicochemical property of Avecmer2-liposomes

Liposome	Size (nm)	ζ-potential (mV)
1mol% PEG_{2k}- liposome	154.9	-15.2
2.5mol% PEG_{2k}- liposome	149.9	-15.8
5mol% PEG_{2k}- liposome	141.6	-19.4
1mol% PEG_{5k}- liposome	145.7	-12.6
2.5mol% PEG_{5k}- liposome	140.3	-10.7
5mol% PEG_{5k}- liposome	127.4	-10.5

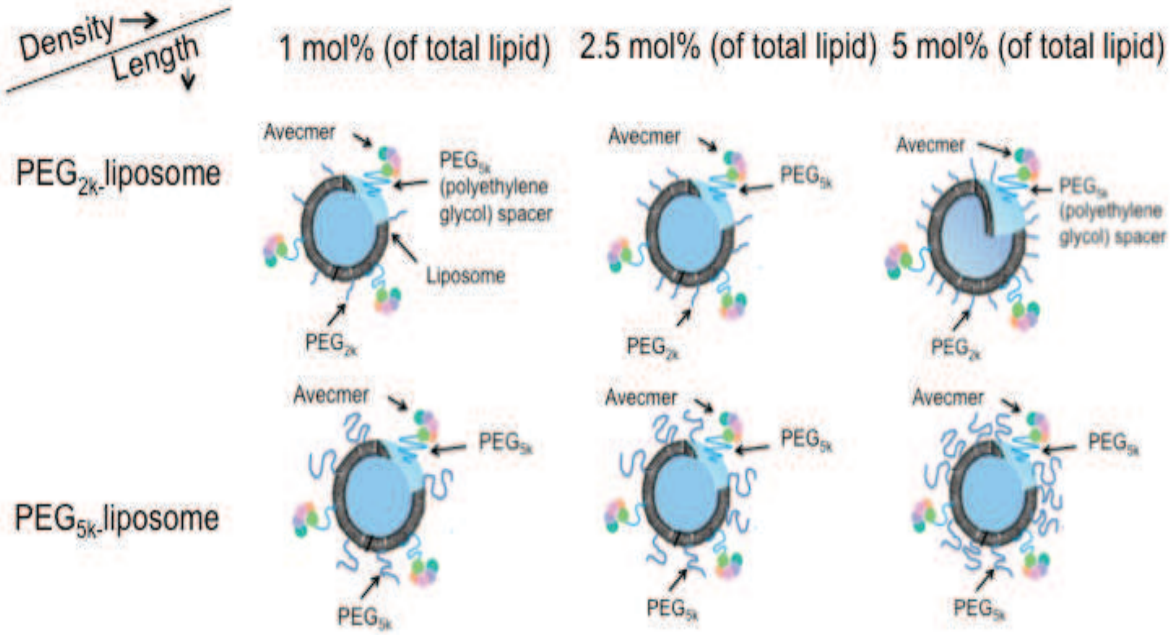

Figure 4.15: Preparation of Avecmer-modified liposomes for optimization.

4.10. *In vivo* targeting of aptamer modified liposomes (Avecmer1-liposome and Avecmer2-liposome) to adipose vasculature

To address the rational design of targeted drug delivery system, *in vivo* behavior of nanoparticles is an important issue. The purpose of this study was to optimize the liposomal composition for targeting to adipose vasculature *in vivo*.

In the previous study of our laboratory, optimization of Pep-liposome for *in vivo* targeting capability was carried out with three types of liposomal composition: Pep-PEG_{2k}- NP, Pep- PEG_{5k}- NP and PTNP. Among these three types of liposome PTNP showed the highest accumulation in the blood vessel of adipose tissue and lowest accumulation in liver. In PTNP, the combination of PEG_{5k}- DSPE (1.25 mol%) and PEG_{2k}- DSPE (1 mol%) was used.

In PTNP, combination of PEG_{5k}- DSPE (1.25 mol%) and PEG_{2k}- DSPE (1 mol%) was used for the surface modification of Pep-liposome (PTNP) for active target to adipose vessels [92]. Whereas, PEG_{5k}- DSPE was used to conjugate peptide ligand on liposome surface and PEG_{2k}- DSPE was remain free. Targeting capability of other two types of liposome [92] was also examined. From this study, it was clear that free PEG on the liposomal surface play an important role for target binding.

Therefore, to optimize the liposomal composition of the Avecmer1-liposome and Avecmer2-liposome for targeting adipose ECs *in vivo*, on the basis of prototype liposome (1mol% PEG_{2k}-liposome) we prepared six types of liposomes considering different PEG length and density.

To endorse the targeting effect *in vivo*, the feasibility of aptamer-modified liposomes was assessed. After systemic administration of rhodamine-loaded of these

liposomes (rhodamine dose: 0.15 μmol/kg) to normal mice, the accumulation of the liposomes to adipose tissue was observed by CLSM. From the tissue observation, it was found that the 5 mol% PEG_{5k}-liposome showed the highest accumulation in adipose tissue (**Figure 4.16 (a), Figure 4.17 (a)**).

To further verify the findings as strong evidence, we quantify the liposomes and the distribution of the liposomes in the unit area (**Figure 4.16 (b, c)** and **Figure 4.17 (b, c)**). The quantitative measurement also presented that the 5mol% PEG_{5k}-liposome exhibited the highest accumulation in adipose tissue.

Thus result demonstrated that longer PEG-chain and higher density offer higher flexibility to exclude steric hindrance for target recognition, which increase ligand-receptor interaction.

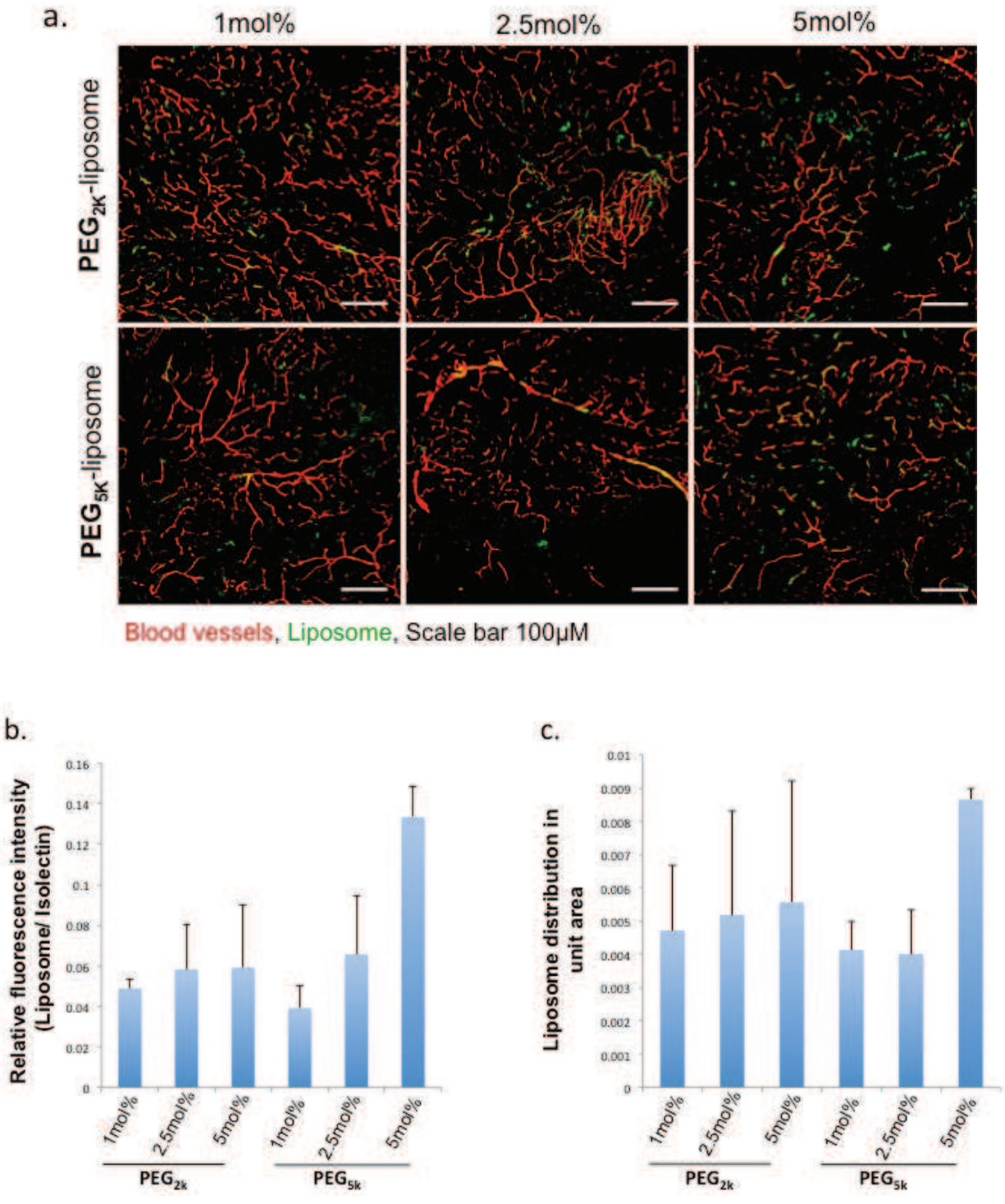

Figure 4.16: *In vivo* targeted delivery of Avecmer1-liposomes to adipose vessels in normal mice. **(a)** Accumulation of targeted six types of liposome in adipose tissue. Normal mice were i.v.-injected with rhodamine-loaded Avecmer1 modified 1mol%

PEG_{2k}-liposome, 2.5mol% PEG_{2k}-liposome, 5mol% PEG_{2k}-liposome, 1mol% PEG_{5k}-liposome, 2.5mol% PEG_{5k}-liposome and 5mol% PEG_{5k}-liposome (green). To visualize blood vessels, 50 μg of FITC-GSIB4 (red) was also i.v.-injected 30 min prior to tissue processing. At 15 h after administration, the adipose tissue was imaged by CLSM. Bars represented 100 μm.

(b) Quantification of liposomes into adipose tissue. Green fluorescence of liposomes accumulated in adipose tissue was normalized to the red fluorescence of blood vessels for quantification.

(c) Quantification of the distribution of Avecmer1-liposomes in adipose tissue. Green fluorescence of liposomes accumulated in adipose tissue was quantified per unit area.

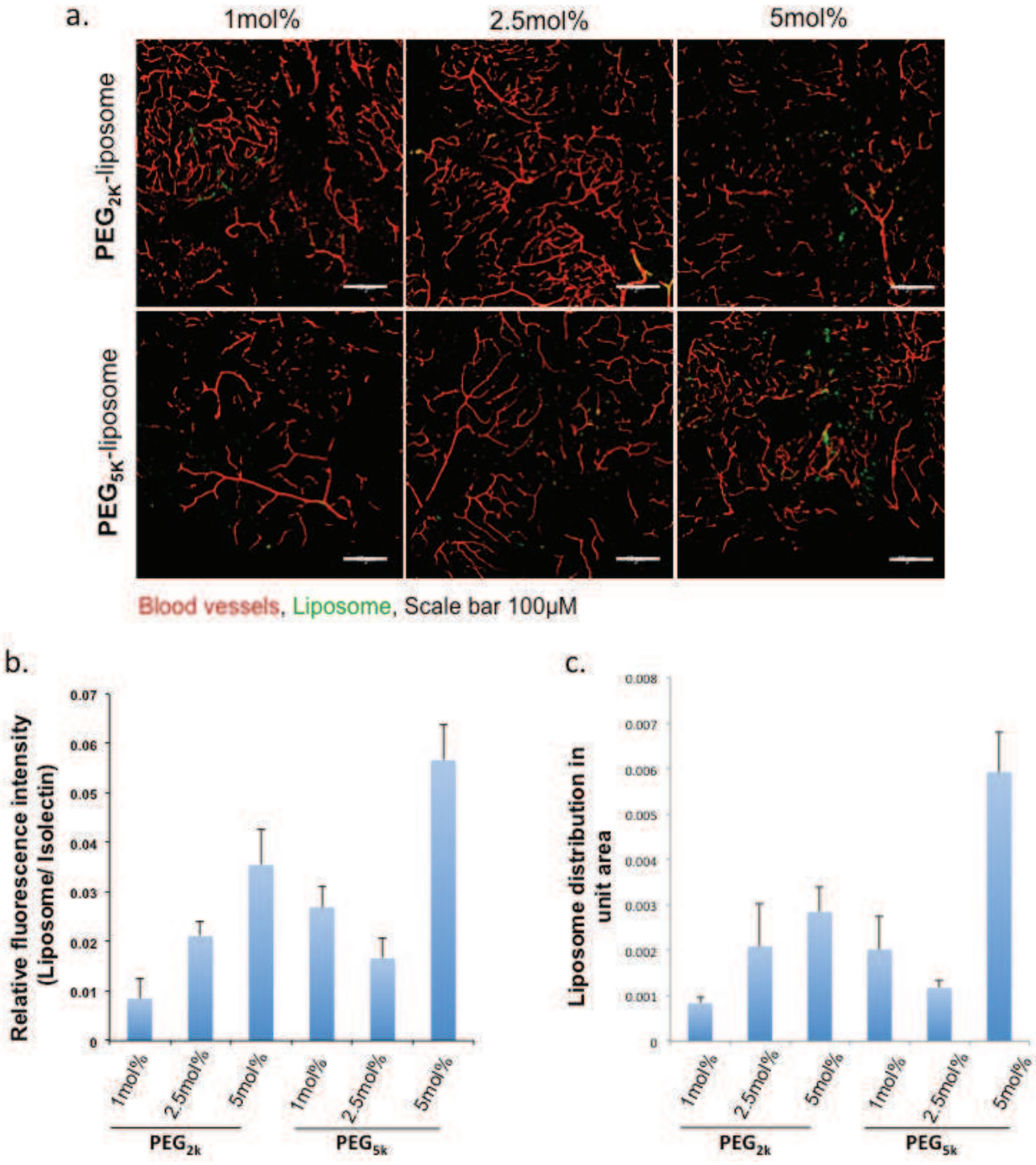

Figure 4.17: *In vivo* targeted delivery of Avecmer2-liposomes to adipose vessels in normal mice. **(a)** Accumulation of targeted six types of liposome in adipose tissue. Normal mice were i.v.-injected with rhodamine-loaded Avecmer2 modified 1mol%

PEG_{2k}-liposome, 2.5mol% PEG_{2k}-liposome, 5mol% PEG_{2k}-liposome, 1mol% PEG_{5k}-liposome, 2.5mol% PEG_{5k}-liposome and 5mol% PEG_{5k}-liposome (green). To visualize blood vessels, 50 μg of FITC-GSIB4 (red) was also i.v.-injected 30 min prior to tissue processing. At 15 h after administration, the adipose tissue was imaged by CLSM. Bars represent 100 μm.

(b) Quantification of liposomes into adipose tissue. Green fluorescence of liposomes accumulated in adipose tissue was normalized to the red fluorescence of blood vessels for quantification.

(c) Quantification of the distribution of Avecmer2-liposomes in adipose tissue. Green fluorescence of liposomes accumulated in adipose tissue was quantified per unit area.

Chapter 5

Discussion

5
Discussion

Obesity and its consequences have become a major health problem, over the last decades [62]. It increases the risk of multiple conditions and negatively affects physical functioning, vitality, and general quality of life [63, 64]. Effective and safe drug and delivery system is not available in obesity treatment. It has been reported that angiogenesis have a crucial role in the modulation of adipogenesis and obesity[65, 66]. Several anti-angiogenic molecules have been used to control obesity but lacking of active targeting it produce undesired toxicity to healthy tissues. To gain cell-specific uptake and to reduce off-target effects, strategies for selective drug deliveries are desirable. Regarding this strategy into concern, currently ligand-based targeted drug delivery to adipose endothelial cell has been introduced for highly effective and safe treatment of obesity [57, 67].

As already mentioned in the introduction, the peptide ligand (KGGRAKD) conjugated proapoptotic sequences (Adipotide) successfully controlled obesity in mouse model. Another promising delivery approach deals with adipose vasculature targeted-nanocarrier system (PTNP) utilizing the peptide ligand demonstrated more effective, efficient and safe therapy for obesity in mice via a proapoptotic peptide/protein-loaded PTNP.

So far, only one peptide ligand has been identified against adipose ECs to specifically escort cargo molecules for obesity therapy. Thus identification of new ligand of adipose ECs and development of targetd-nanocarrier coupled with ligand would be a very attractive strategy for cell- specific delivary and therapy.

Thus, in this study, to develop a novel adipose vasculature-targeted delivery system, we identified nucleic acid aptamers, which can specifically recognize the adipose vascular endothelial cells, and applied the identified aptamer as a ligand for targeted drug delivery system.

Aptamers are short single-stranded oligonucleotides ligands comprise a promising, emerging and attractive class of targeting molecules, being able to bind with high affinity and specificity to protein or non-protein targets by folding into complex secondary and tertiary structures [31, 32].

They have ability to discriminate between closely related targets. Regarding these issues, aptamers are considered as alternative to antibodies for *in vivo* cell recognition. Owing to their relatively small size in comparison to antibodies, they are better suited for rapid target tissue penetration and blood clearance. These properties indicate a great potential of aptamers as targeting agents [34-36, 68].

Aptamers for specific targets are identified using SELEX, starts with complex aptamer libraries consisting of pool sizes of 10^{12}–10^{15}. To facilitate in vitro selection of adipose ECs aptamers we used the cell-based SELEX method, a modification of the usual SELEX technique using live cells (**Figure 4.1**). The technique involved

the use of primary cultured adipose ECs isolated from 9 or 10 weeks male C57BL/6J mice, rather than establish cell lines as a target to isolate specific molecular probes or molecular ligands. Flow cytometry binding assays of the isolated 1st round aptamers confirms that selection procedure was working (**Figure 4.3 (a)**). Flow cytometry data also confirms the enrichment of aptamers in different round of selections. During the selection process, we included some modifications that enhanced the success of the project. Changing of selection condition and cell numbers during selections revealed the saturation of aptamers to target cells within 6th to 9th rounds (**Figure 4.3 (d-e)**) [68].

We also included a negative selection after 9th round, when we were confident that sufficient enrichment of binding pools had been produced (**Figure 4.3**). Here our interpretation was to remove non-specific aptamers, which have ability to bind with ECs of other organs/tissues and to confirm the targeting capability of desired aptamers *in vivo*. For the counter selection, we used *in vivo* SELEX with positive selection and succeed to isolate our desired aptamers (**Figure 4.4 and Figure 4.5**). Selection is a continuous and repetitive process, and results in the production of high affinity targets from random oligonucleotide pools.

Combination of cell-SELEX and *in vivo* SELEX revealed very high-frequented aptamers (**Table 4.1**). Among 92 clones, we selected Seq1 and Seq2 due to their higher frequency. Our concern to select these two aptamers was that the target receptors of these two aptamers are expressed on cell surface with very high amount compare to other candidates. The more receptors expressed on the cell surface is better to deliver cargo molecules into the cells.

Next to assess the targeting capability of both Seq1 and Seq2 *in vitro* and *in vivo* we could exhibit the binding assay through flow cytometry and polymeric chain reaction (**Figure 4.7 and Figure 4.8**). As a negative control, we used a fluorescently tagged random ssDNA pools.

For minimization of the Seq1 and Seq2, we took into account the removal of primer regions from both sides of full-length aptamers (central region of aptamer flanked by two primer region). Generally it is expected that primer regions do not contribute for target binding and secondary structure formation. But some reports show the importance of primer for structure formation and target binding [69, 70]. Binding analysis from flow cytometry confirms that primers are not important for binding to adipose ECs (**Figure 4.9**). These shortened versions of Seq1-40 and Seq2-40, named Avecmer1 and Avecmer2 respectively have been used for the preparation of targeted drug delivery system.

Recently, nanocarrier-based drug delivery system has received powerful attention due to their unique physical, chemical and biological properties. Nanocarriers, for the clinical applications must have to be biocompatible (able to match with a biological system without producing immune response or any negative effects) and nontoxic [71]. For *in vivo* applications, nanoparticles with a diameter of 80–300 nm are generally accepted due to their optimal physicochemical and biological properties [72].

It is now well recognized that liposomes are the widely used nanocarrier for drug delivery system. They are composed of natural or synthetic lipids bilayers consisting

of an aqueous core and capable to deliver both lipophilic to the site of action [30]. However, surface of liposome can be modified with any targeting moieties (antibodies, folate, peptides and nucleic acids) to deliver drugs safely and effectively to the target site [73- 79].

Regarding the targeting of adipose vessels with the goal of controlling obesity, previously our laboratory established a liposomal carrier system modified by a peptide ligand (PTNP) that could accumulates in adipose vessels selectively. And to establish the advantageous effect of nanoparticle-targeted therapeutics, a comparative study was performed with drug-loaded targeted-nanocarrier (PTNP) and drug conjugated targeted ligand (Adipotide). Study revealed that the drug loaded nanocarrier system could reduce obesity in mice efficiently and successfully than the conjugated drug [58]. The release of a drug from liposomes depends on the liposome composition, and the surrounding environment [80].

Therefore, to prepare Avecmer-modified liposome, we considered the composition of liposome used in PTNP and took it as model carrier. For the development of aptamer-based drug delivery system, first we synthesized aptamer conjugated PEG-lipid (Avecmer- PEG_{5k}- DSPE). In this synthesis, Avecmer1 and Avecmer2 were conjugated with NHS- PEG5k- DSPE through a stable ester bond under physiological condition. So that, the ligand would not dissociate from the liposome in the systemic circulation [81] meeting important requirement for a stable targeted delivery system.

The aptamer modified liposome for a ligand-based targeted delivery system was prepared by attaching ligands at the PEG terminus on the liposome [58] (**Figure 4.11**). This is more effective than directly attaching ligands to the surface of a PEG-containing liposome, since PEG chains interfere with both the coupling of ligands to the lipid bilayer and the interaction of these ligands with the intended biological targets. Therefore, we attached ligands to the distal end of PEG chains to overcome this drawback. These ligands coupling to the PEG terminus does not cause any interference with the binding of ligands to their respective recognition molecules. According to previous study, we also use malemide- PEG_{2k}-DSPE for the surface modification of liposome [58].

The efficiency of the Avecmer1-liposome and Avecmer2-liposome was estimated by evaluation of the cellular uptake study with the target cells. Pep-liposome and PEG-liposome were used as positive control and negative control, respectively. As a result, it was found that Avecmer-modified liposomes (Avecmer1-liposome and Avecmer2-liposome) showed a remarkable enhancement in cellular uptake compared to PEG-liposome in adipose ECs (**Figure 4.12**). But the internalization efficiency of Avecmer-modified liposomes were lower than the Pep-liposome. As shown in **Figure 4.12**, PEGylation on the surface of the liposome (PEG-liposome) had a slight inhibitory effect on cellular uptake, indicating that PEGylation generates an aqueous layer on the surface of the liposome which inhibited the interaction of liposome with the cell surface. Different cellular uptake of Avecmer-liposomes and Pep-liposome might be explained by two ways, either expressions of the target

molecules of aptamers are lower than that of peptide ligand on adipose ECs or the binding capability of Avecmer-liposomes are lower than Pep-liposome. To confirm the possibilities next we evaluated the targeting ability of the prepared liposomes to adipose ECs *in vivo*. All the prepared liposomes were systemically administered into mice and adipose tissue was observed though confocal microscopy. After evaluation of confocal images, it was found that the intensity of rhodamine-loaded both Avecmer1-liposome and Avecmer2-liposome was higher than PEG-liposome (**Figure 4.13**). The most interesting point here is, the intensity of rhodamine-loaded Pep-liposome was lower than both Avecmer1-liposome and Avecmer2-liposome, totally reverse result of *in vitro* study (**Figure 4.13**). The *in vivo* distribution data forcefully demonstrated that the homing capability of Avecmer1-liposome and Avecmer2-liposome is higher than Pep-liposome *in vivo*. This result also revealed that the receptor expressions of both aptamers are highly differing in *in vivo* and *in vitro*. In this study to confirm the selectivity of aptamer-liposomes, we also evaluate the accumulation of liposomes in liver and spleen. Findings showed that accumulation of both Avecmer1-liposome and Avecmer2-liposome was observed in liver and spleen, but that was similar to Pep-liposome and PEG-liposome (**Figure 4.14**). From this study we can conclude that our identified aptamers have efficient homing capability to adipose vasculature.

In the preparation of aptamer-modified liposome we have used the same composition of liposome used in previous study of peptide-liposome (PTNP). In this study, we only replace the peptide ligand with our identified aptamers (Avecmer1

and Avecmer2). However, the question of whether this composition is the best one for aptamer-modified liposome to bind with target *in vivo*. Moreover, to address the rational design of targeted drug delivery system, *in vivo* behavior of nanoparticles is an important issue. Therefore, next we optimize the liposomal composition for increasing the targeting ability aptamer to adipose vessel.

In designing an effective targeted nanocarrier, the most critical challenge is to deliver the therapeutic drugs to desired site of action specifically with maximum therapeutic effects and little or no interaction with non-target cells/tissues. Intensive effort has been made so far to achieve these challenges by considering the important factors responsible for the fate of nanocarriers in circulation.

As it is well known that nanocarriers are considered as foreign particles for the body defense system and they undergo into serum opsonization and sometimes undergo quick elimination before completion of their functions. Thus the prerequisite demand of effective therapy is to increase the longevity of nanocarrier in the circulation [82- 84].

To achieve better targeting effect for targeted-drugs and drug carriers, prolonged circulation is helpful due to sustain more time for their interaction with target [85].

Surface modification of nanocarrier with PEG, is a powerful approach to regulate their *in vivo* longevity properties and biological behavior. The surface coating with PEG provides steric stabilization of nanocarriers by forming hydrophilic layer on surface that prevent the drug carrier interaction with opsonins and their fast capture by reticuloendothelial system (RES) [86- 88].

The role of PEG in targeted drug delivery system is less clear. In general targeted drug delivery system, targeting ligand are grafted on the nanocarrier surface via PEG spacer, where an aqueous phase is loaded into therapeutics such as chemotherapeutics, therapeutic peptides or genes in the same nanoparticles. The PEG provides the space between the ligands and the surface of nanoparticles, which reduces the steric hindrance for the recognition of the ligand to target receptor [89]. Moreover, length of the PEG may also play a role in ligand receptor interaction [90, 91]. However, targeting ligand sometimes decrease the biostability of nanoparticle *in vivo* by altering the physicochemical properties of carrier that may assume to obscure the advantages of PEGylation accelerated clearance of ligand-linked nanoformulations.

In the previous optimization study of peptide-modified nanocarrier, length of PEG was taken into consideration. The combined modification of PEG_{5k} and PEG_{2k} on liposomal surface presented the best target binding *in vivo*, whereas PEG_{5k} was used for ligand conjugation and PEG_{2k} was free on the liposome surface. As a result, PEG length and free PEG on liposome surface played an important role for target binding[92].

To enhance the targeting capability of the Avecmer-liposome, we considered density and length of PEG on the surface of liposome. For *in vivo* applications, we designed six types of targeted liposomes (**Figure 4.15**) and compared the targeting ability of these liposomes to adipose vessels by confocal-based observations (**Figure 4.16 and**

Figure 4.17). Although these liposomes were modified with the same amount of ligand and showed similar physicochemical properties, including size and ζ-potential (**Table 4.3** and **Table 4.4**), their targeting activities were substantially different after systemic injection.

In case of both Avecmer1-liposome and Avecmer2-liposome (**Figure 4.16** and **Figure 4.17**) 5mol% PEG_{5k}- liposome showed the highest accumulation in adipose vessels. Quantitative measurement of confocal images also demonstrates the same result. These results suggest not only ligand but also the surface biostabilizing activity of PEG and the length of spacer is important factors for maximizing the targeting of a ligand to a target *in vivo*. In this study, we exhibited that liposomes modified with longer PEG and highest density had the best accumulation in adipose vessels, however, further investigations will be needed to determine the detailed molecular basis.

Chapter 6

Conclusion

6
Conclusion

Here we report on novel targeted drug delivery system for adipose vasculature based on our identified novel nucleic acid aptamers that can function successfully in both *in vitro* and *in vivo*.

This study is the first report on the combined use of whole-cell SELEX and *in vivo* SELEX to identify nucleic acid aptamers. The advantages of cell-SELEX on culture dish, exposes, no need for a detailed study of the target before the start of the selection; aptamers bind to the target in their original conformation. Study reveals that the flow cytometry assays can be used for both the progression of selection and, affinity analysis. As shown in the results, sequences after *in vivo* SELEX have binding ability to target cells and ability to accumulate in target vessels. Moreover, without any types of chemical modifications, they are very stable in body fluid. This opens the new era of identification for targeting nucleic acid ligands for *in vivo* application. However, both Avecmer1 and Avecmer2 have higher binding affinity to target cells and both can be used as targeting ligand for adipose vasculature.

By using the high affinity DNA aptamers, we successfully developed the targeted nanoparticle. This active targeted carrier can internalize into the target cells *in vitro* that is lower than the peptide ligand. But this has the ability of higher accumulation in the target tissue than the peptide ligand *in vivo*. We may propose that our identified aptamers have higher targeting capability to adipose vasculature.

The role of PEG has proven crucial in the evolution of drug delivery systems. The findings presented herein also show that the PEGylation of targeted liposomes can improve the targeting efficiency *in vivo*. In case of both Avecmer1-liposome and Avecmer2-liposome, 5mol% PEG_{5k}-liposome is the best liposomal composition for target binding. In addition, both liposomes can deliver an aqueous phase marker to the target that mimics the delivery of small molecular drugs, proteins, peptides and nucleic acid.

Taken together, the findings provide a proof concept of novel targeted carrier system for adipose vasculature. In near feature, this work may offer a paradigm shift in the development of anti-obesity drug for the treatment and control of obesity.

Chapter 7

References

7

References

1. Haslam, DW. James, WPT. Obesity. *Lancet,* **2005**; 366, 1197-209.
2. Lau, DCW, Douketis, JD, Morrison, KM, Hramiak IM, Sharma AM, Ehud Ur. Canadian clinical practice guidelines on the management and prevention of obesity in adults and children. **2006**, CMAJ2007; 176:S1-130.
3. The World Health Report, *WHO*. **2000**, 9.
4. Masuzaki, H., Paterson, J., Shinyama, H., Morton, N.M., Mullins, J.J., Seckl, J.R., Flier J.S. A transgenic model of visceral obesity and the metabolic syndrome. *Science*, **2001**, 294, 5549, 2166–2170.
5. Kopelman, P.G. Obesity as a medical problem. *Nature*, **2000**, 404, 6778, 635–643.
6. Spiegelman, B.M., Flier, J.S. Obesity and the regulation of energy balance. *Cell*, **2001**, 104, 4, 531–543.
7. Fontaine, K.R., Redden, D.T., Wang, C., Westfall, A.O., Allison, D.B. Years of life lost due to obesity. *JAMA*, **2003**, 289, 2, 187–193.
8. Pollack, A. A.M.A. Recognizes Obesity as a Disease. *New York Times*. Archived from the original on June 18, **2013**.
9. Weinstock, M. The Facts About Obesity. *H&HN*. American Hospital Association, June 21, **2013**.

10. Lau, DC., Douketis, JD., Morrison, KM., Hramiak, IM., Sharma. AM., Ur E. Canadian clinical practice guidelines on the management and prevention of obesity in adults and children summary, *CMAJ,* **2006***,* 176 ,8, S1–13.

11. Shick, SM., Wing, RR., Klem, ML., McGuire, MT., Hill, JO., Seagle, H. Persons successful at long-term weight loss and maintenance continue to consume a low-energy, low-fat diet. *J Am Diet Assoc*. **1998**, 98, 4, 408–13.

12. Tate, DF., Jeffery, RW., Sherwood, NE., Wing, RR. Long-term weight losses associated with prescription of higher physical activity goals. Are higher levels of physical activity protective against weight regain? *Am. J. Clin. Nutr.,* **2007***,* 85, 4, 954–959.

13. Strychar, I. Diet in the management of weight loss. *CMAJ,* **2006***,* 174, 1, 56–63.

14. Wing, RR., Phelan, S. *Am. J. Clin. Nutr.,* **2005***,* 82, 207S–273S.

15. Haskell, WL., Lee, IM., Pate, RR. Physical activity and public health: updated recommendation for adults from the American College of Sports Medicine and the American Heart Association. *Circulation,* **2007***,* 116**,** 9, 1081–93.

16. Cooke, D., Bloom, S. The obesity pipeline: current strategies in the development of anti-obesity drugs. *Nat. Rev. Drug Discov*., **2006**, 5, 919–931.

17. Sargent, B. J., Moore, N. A. New central targets for the treatment of obesity. *Br. J. Clin. Pharmacol*., **2009**, 68, 852–860.

18. Padwal, RS., Majumdar, SR., Drug treatments for obesity: orlistat, sibutramine, and rimonabant. *Lancet*. **2007**, 369, 71–77.

19. Lettner, A., Roden, M. Ectopic fat and insulin resistance. *Curr. Diabetes Rep.,* **2008,** 8, 3, 185-191

20. Christiaens, V., Lijnen, H.R. Angiogenesis and development of adipose tissue. *Molecular and Cellular Endocrinology*. **2010**, 318, 2–9

21. Garg, A., Kokkoli, E. Characterizing particulate drug-delivery carriers with atomic force microscopy. *IEEE Engineering in Medicine and Biology Magazine*, **2005**, 24**,** 1, 87-95.

22. Muller, R.; Keck, C. Challenges and solutions for the delivery of biotech drugs – a review of drug nanocrystal technology and lipid nanoparticles. *Journal of Biotechnology,* **2007***,* 113, 151–170.

23. Langer, R. Drug delivery and targeting. *Nature*, **1998**. 392, 5- 10.

24. Torchilin, V.P. Drug targeting. *European Journal of Pharmaceutical Sciences*, **2000**, 11, S81-S91.

25. Sinha, R., Kim, GJ., Nie, S., Shin, DM., Nanotechnology in cancer therapeutics: bioconjugated nanoparticles for drug delivery. *Molecular Cancer Therapeutics*, **2006**. 5**,** 8, 1909-1917.

26. Bendasa, G., Krausea, A., Bakowskya, U., Vogela, J. Rotheb, U. Targetability of novel immunoliposomes prepared by a new antibody conjugation technique. *International Journal of Pharmaceutics*, **1999**. 181,1, 79-93.

27. Garg, A., Tisdale, AW., Haidari, E., Kokkoli, E. Targeting colon cancer cells using PEGylated liposomes modified with a fibronectin-mimetic peptide. *International Journal of Pharmaceutics*, **2009**. 366, 1-2, 201-210.

28. Lundberg, B., Hong, K. Papahadjopoulos, D. Conjugation of apolipoprotein B with liposomes and targeting to cells in culture. *Biochim Biophys Acta*. **1993**. 1149, 2, 305-312.

29. Farokhzad, O.C., Cancer nanotechnology: drug encapsulated nanoparticle-aptamerbioconjugates for targeted delivery to prostate cancer cells. *Ejc Supplements*, **2005**. 3, 2, 229-230.

30. Gulati, M., Grover, M., Singh, S. Lipophilic drug derivatives in liposomes. *Int J Pharm*. **1998**;165, 129–168.

31. Ellington, A.D., Szostak, J. W. In vitro selection of RNA molecules that bind specific ligands. *Nature*, **1990**, 346, 6287, 818-822.

32. Tuerk, C., Gold, L. Systemic evolution of ligands by exponential enrichment: RNA ligands to bacteriophage T4 DNA polymerage. *Science*, **1990**, 249, 505-510.

33. Tanvtian, B., Ducongé, F., Boisgard, R., Dollé. F. In- vivo imaging of oligonucleotidicaptamers. *Methods in Molecular Biology*, **2009**, 535, 241-259.

34. Perkins A.C., Missailidis, S. Radiolabelled aptamers for tumour imaging and therapy. *The Quarterly Journal of Nuclear Medicine and Molecular imaging*, **2007**, 51, 4, 292-296.

35. Esposito, C.L., Catuogno, S.; de Franciscis, V., Cerchia, L. New insight into clinical development of nucleic acid aptamers. *Discov. Med.,* **2011**, 11, 61, 487-496.

36. Keefe, A.D., Cload, S.T. SELEX with modified nucleotides. *Current Opinion in Chemical Biology,* **2008**, 12, 4, 448-456.

37. Golden, M.C., Collins, B.D., Willis, M.C., Koch, T.H. Diagnostic potential of Photo SELEX-evolved ssDNA aptamers. *J. Biotechnol*., **2000**, 81, 167–178.

38. Cox, J.C., Ellington, A.D. Automated selection of anti-protein aptamers. *Bioorg. Med. Chem.,* **2001**, 9**,** 2525–2531.

39. Kim, S.J., Kim, M.Y., Lee, J.H., You, J.C., Jeong, S. Selection and stabilization of the RNA aptamers against the human immune deficiency virus type-1 nucleocapsid protein. *Biochem. Biophys. Res. Commun.* **2002**, 291**,** 925–931.

40. Bruno, J.G., Kiel, J.L. Use of magnetic beads in selection and detection of biotoxin aptamers by electrochemiluminescence and enzymatic methods. *Biotechniques,* **2002**, 32**,** 178–183.

41. Bryant, K.F., Cox, J. C., Wang, H., Hogle, J. M., Ellington A. D., Coen D. M., Binding of herpes simplex virus-1 US11 to specific RNA sequences. *Nucleic Acids Res.* **2005**, 33**,** 6090–6100.

42. Noma, T., Ikebukuro, K., Sode, K., Ohkubo, T., Sakasegawa, Y., Hachiya, N., Kaneko, K. A screening method for DNA aptamers that bind to specific, unidentified protein in tissue samples. *Biotechnol. Lett.* **2006**, 28**,** 1377–1381.

43. Shamah, S.M., Healy, J.M., Cload, S.T. Complex target SELEX. *Acc. Chem. Res.* **2008**, 41**,** 130–138.

44. Tang, J., Parekh, P., Turner, P., Moyer, RW., Tan, W. Generating aptamers for recognition of virus–infected cells. *Clin Chem.***2009**, 55, 813–822.

45. Sefah, K., Meng, L., Lopez-Colon, D., Jimenez, E., Liu, C., Tan, W. DNA aptamers as molecular probes for colorectal cancer study. *PLoS One*, **2010**, 5: 1-14.

46. Zhao, Z., Xu, L., Shi, X., Tan, W., Fang, X., Shangguan. D., Recognition of subtype non- small cell lung cancer by DNA aptamers selected from living cells. *Analyst*. **2009**, 134, 1808–1814.

47. Sefah, K., Tan, ZW., Shangguan, D., Chen, H., Lopez-Colon, D., Li, Y., Parekh, P., Martin, J., Meng, L., Phillips, JA., Kim, YM., Tan, WH. Molecular recognition of acute myeloid leukemia using aptamers. *Leukemia,* **2009**, 23, 235–244.

48. Daniels, DA., Chen, H., Hicke, BJ., Swiderek, KM., Gold, L. Atenascin-C aptamer identified by tumor cell SELEX. *Proc. Natl. Acad. Sci. U S A*. **2003**, 100, 15416– 15421.

49. Ferreira, CSM., Cheung, MC., Missailidis, S., Bisland, S., Gariepy, J. Phototoxic aptamers selectively enter and kill epithelial cancer cells. *Nucleic Acids Res*. **2009**, 37, 866–876.

50. Lysons, S. K. Advances in imaging mouse tumour model in- vivo. *Journal of pathology*, **2005**, 205, 2, 194-205

51. O'Reilly, MS., Holmgren, L., Shing, Y., Chen, C., Rosenthal, RA., Moses, M., Lane, WS., Cao, Y., Sage, EH., Folkman, J. Angiostatin: a novel angiogenesis inhibitor that mediates the suppression of metastases by a Lewis lung carcinoma. *Cell,* **1994**, 79, 315–328.

52. O'Reilly, MS., Boehm, T., Shing, Y., Fukai, N., Vasios, G., Lane, WS., Flynn, E., Birkhead, JR., Olsen, BR., Folkman, J. Endostatin: an endogenous inhibitor of angiogenesis and tumor growth. *Cell,* **1997**, 88, 277–285.

53. Brakenhielm, E., Cao, R., Gao, B., Angelin, B., Cannon, B., Parini, P., Cao, Y. Angiogenesis inhibitor, TNP-470, prevents diet-induced and genetic obesity in mice. *Circ. Res.,* **2004**, 94, 1579–1588.

54. Rupnick, MA., Panigrahy, D., Zhang, CY., Dallabrida, SM., Lowell, BB., Langer, R., Folkman, MJ. Adipose tissue mass can be regulated through the vasculature. *Proc. Natl Acad. Sci. USA,* **2002**, 99, 10730–10735.

55. Tam, J., Duda, DG., Perentes, JY., Quadri, RS., Fukumura, D., Jain, RK. Blockade of VEGFR2 and not VEGFR1 can limit diet-induced fat tissue expansion: role of local versus bone marrow-derived endothelial cells. *PLoS ONE,* **2009**, 4, e4974.

56. Fukumura, D., Ushiyama, A., Duda, DG., Xu, L., Tam, J., Chatterjee, KK., Garkavtsev, I., Jain, RK. Paracrine regulation of angiogenesis and adipocyte differentiation during*in vivo* adipogenesis. *Circ. Res.,* **2003,** 93, e88–97.

57. Kolonin, MG., Saha PK., Chan L., Pasqualini, R., Arap, W. Reversal of obesity by targeted ablation of adipose tissue. *Nature Medicine,* 2004, 10, 625 – 632.

58. Hossen, M.N., Kajimoto, K., Akita, H., Hyodo, M., Harashima, H. A comparative study between nanoparticle-targeted therapeutics and bioconjugates as obesity medication. *J. Control. Release,* **2013**, 171, 104-112.

59. Kajimoto, K., Hossen, M.N., Hida, K.,Ohga, N., Akita, H., Hyodo, M., Hida, Y., Harashima, H. Isolation and culture of microvascular endothelial cells from murine inguinal and epididymal adipose tissue. *J.Immunol. Methods.***2010,** 357 (1-2), 43–50.

60. Szoka, FJR., Papahadjopoulos, D. Procedure for preparation of liposomes with large internal aqueous space and high capture by reverse-phase evaporation. *Proc. Natl Acad. Sci. USA,* **1978**, 75, 4194–4198.

61. Nishimura, S., Manabe, I., Nagasaki, M., Hosoya, Y., Yamashita, H., Fujita, H., Ohsugi, M., Tobe, K., Kadowaki, T., Nagai, R., Sugiura, S. Adipogenesis in obesity re- quires close interplay between differentiating adipocytes, stromal cells, and blood vessels. *Diabetes*, **2007**, 56, 1517–1526.

62. Hedley, AA., Ogden, CL., Johnson, CL., Carroll, MD., Curtin, LR., Flegal, KM. Prevalence of overweight and obesity among US children, adolescents, and adults 1999–2002. *JAMA*, **2004**, 291, 2847–2850.

63. Kopelman, PG., Obesity as a medical problem. *Nature,* **2000**, 404, 635–643.

64. Roth, J., Qiang, X., Marban, SL., Redelt, H., Lowell, BC. The obesity pandemic: where have we been and where are we going? *Obes Res*, **2004**, 12, S88– 101.

65. Cao, Y. Angiogenesis modulates adipogenesis and obesity. *J. Clin. Invest.,* **2007**, 117**,** 2362–2368.

66. Lijnen, H. R. Angiogenesis and obesity. *Cardiovasc. Res.,* **2008**, 78, 286–293.

67. Hossen, M.N., Kajimoto, K., Akita, H., Hyodo, M., Ishitsuka, T., Harashima, H. Therapeutic assessment of Cytochrome C for the prevention of obesity through endothelial cell-targeted nanoparticulate system. *Molecular Therapy,* 2013, 21, 533-541.

68. Sefah, K., Shangguan, D., Xiong,. X, Donoghue, MB., Tan, W. Development of DNA aptamer using cell-SELEX. *Nat Protoc*, **2010**, 5, 1169–1185.

69. Kaur, H., Yung, L-Y. L. Probing high affinity Sequences of DNA aptamer against $VEGF_{165}$. *Plos one*, **2012**, 7, 2, e31196

70. Nadal, P., Svobodova, M., Mairal, T., O'Sullivan, C. K. Probing high- affinity 11-mer DNA aptamer against Lup an 1 (β- conglutin). *Anal BioanalChem*, **2013,** 405, 29, 9343-9349.

71. Ai, J., Biazar, E., Montazeri, M., Majdi, A., Aminifard, S., Safari, M., Akbari, HR. Nanotoxicology and nanoparticle safety in biomedical designs. *Int J Nanomedicine*, **2011**, 6, 1117–1127.

72. Suri, SS., Fenniri, H., Singh, B. Nanotechnology-based drug delivery systems. *J Occup Med Toxicol*, **2007**, 2, 16.

73. Dharap, SS., Wang, Y., Chandna, P., Khandare, JJ., Qiu ,B. Tumor- specific targeting of an anticancer drug delivery system by LHRH peptide. *Proc. Natl. Acad. Sci USA*, **2005,** 102, 12962–12967.

74. Lee, TY., Lin, CT., Kuo, SY., Chang,. DK, Wu, HC. Peptide-mediated targeting to tumor blood vessels of lung cancer for drug delivery. *Cancer Res,* **2007**, 67, 10958–10965.

75. Chang, DK., Chiu, CY., Kuo, SY., Lin, WC., Lo, A. Antiangiogenic targeting liposomes increase therapeutic efficacy for solid tumors. *.J Bio. lChem.,* **2009**, 284, 12905–12916.

76. Lee,. TY, Wu, HC., Tseng, YL., Lin, CT. A novel peptide specifically binding to nasopharyngeal carcinoma for targeted drug delivery. *Cance.r Res.*, **2004,** 64, 8002– 8008.

77. Park, JW., Hong, K., Kirpotin, DB., Colbern, G., Shalaby, R., Baselga, J., Shao, Y., Nielsen, UB., Marks, JD., Moore, D., Papahadjopoulos, D., Benz, CC. Anti-HER2 immunoliposomes: enhanced efficacy attributable to targeted delivery. *Clin. Cancer. Res.,* **2002**, 8, 1172–1181.

78. Lu, RM., Chang, YL., Chen, MS., Wu, HC. Single chain anti-c-Met antibody conjugated nanoparticles for in vivo tumor-targeted imaging and drug delivery. *Biomaterials,* **2011**, 32, 3265–3274.

79. Pastorino F, Brignole C, Di Paolo D, Nico B, Pezzolo A, Marimpietri, D., Pagnan, G., Piccardi, F., Chilli, M., Longhi, R., Ribatti, D., Corti, A., Allen, TM., Ponzoni, M. Targeting liposomal chemotherapy via both tumor cell-specific and tumor vasculature- specific ligands potentiates therapeutic efficacy. *Cancer. Res,.* **2006,** 66, 10073–10082.

80. Giuberti CDS., Reis, ECO., Rocha, TGR., Leite, EA., Lacerda, RG., Ramaldes, GA., Oliveira, MC. Study of the pilot production process of long-circulating and pH-sensitive liposomes contain- ingcisplatin. *J. Liposome. Res.,* **2011**, 21, 60–69.

81. Nallamothu, R., Wood, GC., Pattillo, CB., Scott, RC., Kiani, MF., Moore, BM., Thoma, LA. A tumor vasculature targeted liposome delivery system for combretastatin A4: design, characterization, and in vitro evaluation, *AAPS Pharm. Sci. Tech.,* **2006**, 7, E32.

82. Moghimi, SM., Szebeni, J. Stealth liposomes and long circulating nanoparticles: critical issues in pharmacokinetics, opsonizations and protein binding properties. *Prog. Lipid. Res.,* **2003**, 42, 463-478.

83. Torchilin, VP., Trubetskoy, VS. New synthetic amphiphilic polymers for steric protection of liposome in vivo. *J. Pharm. Sci.,* **1995b**, 84, 1049-1053

84. Lasic, DD., Martin, FJ. Stealth Liposomes. *CRC Press, Boca Raton*, **1995,** 320.

85. Torchilin, VP., Polymer- coated long- circulating microparticulate pharmaceuticals. *J. Microencapsul*., **1998,** 15, 1-19.

86. Klibanov, AL., Maruyama,, K., Torchilin VP., Huang, L. Amphipathic polyethylenglycols effectively prolonged the circulation time of liposomes. *FEBS Lett*., **1990**, 268, 235-237.

87. Maruyama, K. Effect of molecular weight in amphipathic polyethyleneglycol on prolonging the circulation time of large unilamellar liposomes. *Chem. Pharm. Bull.,* **1991,** 39, 1620-1622.

88. Lasic, DD., Martin, FJ., Gabizon, A., Huang, SK. Papahadjopoulos, D. Sterically stabilized liposomes: a hypothsis on on the molecular origin of the extended circulation times. *Biochim. Biophys. Acta.,* **1991,** 1070, 187-192.

89. Allen, TM., Cullis. PR. Drug delivery systems: Entering the mainstream. *Science*, **2004,** 303, 1818-1822.

90. Yamada, A., Taniguch,i Y., Kawano, K. Design of folate-linked liposomal doxorubicin to its antitumor effect in Mice. *Clin. Cancer Res.,* **2008,** 14, 8161-8168.

91. Gabizon,, A., Horowitz AT., Goren, D. In vivo fate of folate-targeting polyethylene-glycol liposomes in tumor- bearing mice. *Clin. Cancer Res.,* **2003,** 9, 6551- 6559.

92. Hossen, M.N., Kajimoto, K., Akita, H., Hyodo, M., Harashima, H. Vascular-targeted nanotherapy for obesity: Unexpected passive targeting mechanism to obese fat for the enhancement of active drug delivery. *Journal of Controlled Release,* **2012**, 163, 101–110.